

1 Response: We thank the reviewers for thoughtful suggestions and constructive criticism that  
2 have helped us improve our manuscript. We have included responses in blue font below.

3  
4 **Anonymous Referee #1**

5  
6 Through ground-based observations, the authors studied physical and chemical properties of  
7 aerosol particles for 14 selected cases over Metro Manila, Philippines. This kind of ground-based  
8 data analysis is welcomed by both remote sensing folks as well as modelers for CTMs. The  
9 paper is well written. The data analysis part of the paper seems reasonable, as I am not a chemist.  
10 Thus, I rely on other reviewers who have a background in chemistry to fully evaluate the  
11 chemistry portion of the study. Still, I have a few concerns that I hope the authors can address.

12  
13 First of all, for the methodology section, more details are needed. For example, the detection  
14 limits of ground-based observations are included in the supplement. Still, the authors need to  
15 mention uncertainties of other data and models used in the study. For example, precipitation  
16 amounts were obtained from PERSIANN-CCS data, but what is the uncertainty of the dataset?  
17 Also, details for some datasets such as CALIOP Level 2 VFM (version of the dataset, spatial  
18 resolution etc.) need to be provided for the benefit of the readers.

19  
20 Response: While we are unable to provide specific numbers for the uncertainties of some of  
21 datasets, we have added the following text to clarify:

22  
23 “Benefits of PERSIANN-CCS include the data availability at 0.04° x 0.04° spatial resolution,  
24 while uncertainties in the dataset arise from sources such as a lack of bias correction (Nguyen et  
25 al., 2014).”

26  
27 “The CALIOP Level 2 Vertical Feature Mask (VFM) Version 4.20 was used to distinguish  
28 between clear air, clouds, and aerosol (Vaughan et al., 2004). For figures of CALIOP VFM data  
29 in this study, data are plotted at 30 m vertical resolution every 5 km along the satellite ground-  
30 track.”

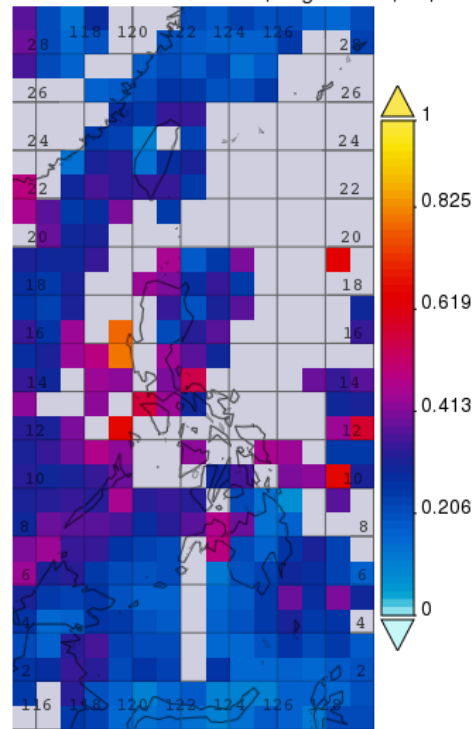
31  
32 The temporal sampling window is different for different cases. While the temporal sampling  
33 window is approximately 2-day for most cases, the temporal sampling window is 5-day for MO4  
34 and 1-day for MO1. Does the difference in temporal sampling window introduce a temporal-  
35 sampling related bias?

36  
37 Response: The initial sets were taken at the very beginning of a year-long sampling campaign.  
38 As these measurements were new to the metro Manila environment, we were unclear of how  
39 long to run the instrumentation for optimal sampling. Therefore, the variations in sample lengths  
40 represent different tests until we settled on a 2-day sampling window. However, for all sets, we  
41 attempted to sample in increments of 24 hrs in order to minimize diurnal influences.  
42 Furthermore, the length of sampling factors into the conversion of the aqueous concentrations to  
43 air-equivalent measurements. Therefore, we believe any differences in measurements due to  
44 varying sampling windows are minimized. We do not feel as though text revisions are needed in  
45 the draft to address this comment.

47 I understood that satellite aerosol retrievals have difficulties over the study region due to cloud  
48 coverage. But it is still useful to provide an aerosol optical depth (AOD) climatology for the  
49 study period (July-Oct. 2018) as well as the spatial distribution of AODs for the selected cases  
50 (e.g. MO7, 11, 12 and 14) using passive-based satellite data such as MODIS or MISR. Such an  
51 analysis will assist their modeling-based analysis (e.g. from NAAPS). This might also help the  
52 authors link their case studies with the aerosol climatology of the region.  
53

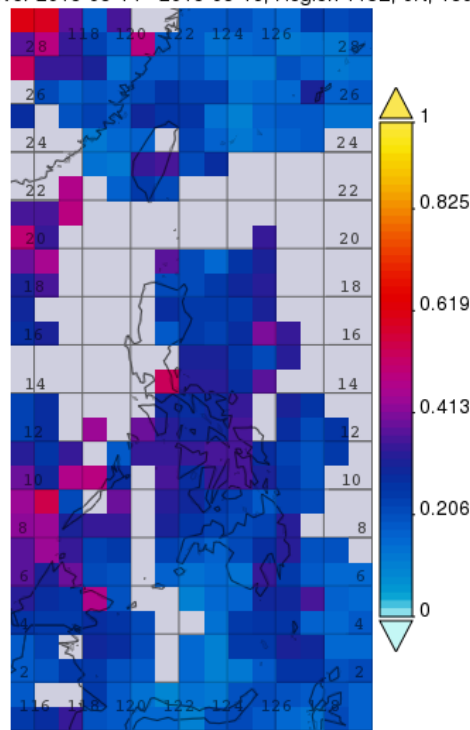
54 **Response:** We have purposefully chosen not to include AOD from passive remote-sensors for the  
55 following reasons. As shown in Figure 1, very high average cloud fractions are found in all of  
56 the sample sets. Therefore, any AOD measurements from passive remote-sensors will either not  
57 have data available or have data with significant clear-sky bias. As an example, we have  
58 included plots here for just the select case of MO7. As is seen for both the MODIS Terra and  
59 MODIS Aqua results, there are significant gaps in the data availability. Furthermore, one  
60 purpose of the paper is to demonstrate the variability in aerosol transport pathways. Therefore,  
61 any climatology of AOD in the region from July-October will remove these nuances and be  
62 subjected to the same clear-sky biasing as described above.  
63  
64

Time Averaged Map of Aerosol Optical Depth 550 nm (Dark Target) daily 1 deg. [MODIS-Terra MOD08\_D3 v6.1]  
over 2018-08-14 - 2018-08-16, Region 115E, 0N, 130E, 30N



65

Time Averaged Map of Aerosol Optical Depth 550 nm (Dark Target) daily 1 deg. [MODIS-Aqua MYD08\_D3 v6.1] over 2018-08-14 - 2018-08-16, Region 115E, 0N, 130E, 30N



66  
67  
68  
69  
70  
71  
72  
73  
74  
75  
76  
77  
78  
79  
80  
81  
82  
83  
84  
85  
86  
87  
88  
89  
90  
91  
92

Speaking of which, I think the linkage between data analysis presented in this study and broader scientific questions is still plausible. For example, how representative are those selected 12 events to different aerosol transport scenarios or to the general aerosol climatology of the region? What are the linkages between the data analysis presented in the study and some broader scientific questions? I hope the authors can add more related discussions.

Response: The 12 events in the study represent the start of a campaign of weekly measurements at the study site that occurred for a full year. Here, we are presenting just the results from the first sets that occurred during the Southwest Monsoon season, into the transition to the Northeast Monsoon. During this time frame, we have identified a few high aerosol events and one low aerosol event, with the remaining cases forming what we are considering the “background conditions.” As shown in the HYSPLIT for these cases in Figure S1, the predominant flow pattern is from the southwest. However, since these are only from one season of measurements and there is a lack of size-resolved aerosol measurements in the region, it is difficult to say with certainty whether this represents the general aerosol climatology for the time frame. Our objective is to highlight potential transport pathways for which we believe we can observe signals in Metro Manila.

In terms of broader scientific questions, we have amended that end of the conclusion to highlight some more relevant discussions and questions that can be addressed in future research:

“These results have important implications for better understanding the aerosol budget and influences in and around the Philippines and SE Asia. Transport of aerosol both into and out of Metro Manila can impact human health, cloud condensation nuclei (CCN) budgets, and radiative

93 forcing in the region. Furthermore, the identification of various tracer species (e.g. K and Rb for  
94 biomass burning) and the impacts of different long-range transport mechanisms have worldwide  
95 applications. In addition, the mixing of different air mass types, resulting in changes in aerosol  
96 characteristics (e.g. enhanced oxalate in emissions from continental regions, enhanced MSA  
97 during periods of biomass burning influence), is a subject that requires more attention on a global  
98 basis. While this work has shown the influence of mixing biomass burning emissions and urban  
99 emissions, from both local and more distant urban centers, additional analysis at the study site  
100 has demonstrated the influences seen from the mixing of sea salt aerosol with other airmasses  
101 (AzadiAghdam et al., 2019). As remote-sensing measurements in this region are notoriously  
102 difficult (e.g. Reid et al., 2009, 2013), in situ and model results lend vital data to address the  
103 questions surrounding characteristics of aerosol that are transported into and out of this highly-  
104 populated region. Measurements from in situ airborne campaigns, such as CAMP2Ex, can  
105 further address the changes in aerosol physicochemical characteristics that occur during long-  
106 range transport and aging in the atmosphere in the region.”

107  
108 AzadiAghdam, M., Braun, R. A., Edwards, E.-L., Bañaga, P. A., Cruz, M. T., Betito, G.,  
109 Cambaliza, M. O., Dadashazar, H., Lorenzo, G. R., Ma, L., MacDonald, A. B., Nguyen, P.,  
110 Simpas, J. B., Stahl, C., and Sorooshian, A.: On the nature of sea salt aerosol at a coastal  
111 megacity: Insights from Manila, Philippines in Southeast Asia, *Atmospheric Environment*, 216,  
112 116922, <https://doi.org/10.1016/j.atmosenv.2019.116922>, 2019.

113  
114 **Anonymous Referee #3**

115 The authors presented their efforts in analyzing local observations collected at the MOUDI  
116 sample site, and tried to attribute the observed changes of water-soluble aerosol to long-range  
117 transport from MC and north East Asia. This is an interest and innovative research as the air  
118 quality in Philippines hasn't been well documented in the published studies. The observations  
119 collected through this study also provided detailed description of the aerosol size distribution,  
120 chemical composition, and temporal changes. The coupling of satellite product, surface  
121 observations, HYSPLIT trajectories, and NAAPS simulations is acceptable, but there are two  
122 major concerns regarding this method:

123  
124 First, the sampling study period is relatively too narrow to justify the description of “high” and  
125 “low” aerosol loading periods, as the concentrate ranges from 2.7 to 13.7 ug/m3, I didn't see  
126 there is significant difference especially considering the wash-out effect of precipitation during  
127 the “low” loading period. It will be better if the authors can present some data or cite from other  
128 studies to briefly describe the year-long trend of aerosol concentration at MOUDI site.

129  
130 Response: We are not attempting to classify high and low loading events for a full annual basis;  
131 rather, our description of the “high” vs. “low” aerosol loading events is within the context of the  
132 sampling time frame (July – October 2018), as stated in the methodology: “For each MOUDI set  
133 (naming convention: MO#), the mass concentration sum of the water-soluble species was  
134 calculated; using this summation, the three high-aerosol loading events were identified (MO7,  
135 MO12, and MO14), as well as the lowest aerosol event (MO11).” Furthermore, we are only  
136 looking at the water-soluble portion of the aerosol, not the total mass, so the overall  
137 concentrations we are working with will be smaller. We have added to the text the following line

138 to highlight the departure from the mean for the identified case studies within our sampling time  
139 frame:

140  
141 “The average  $\pm$  standard deviation of the total-water soluble species measured for the remaining  
142 8 sets not identified in the high or low categories is  $6.99 \pm 2.71 \mu\text{g m}^{-3}$ .”

143  
144 We have also added the following text to the introduction:

145  
146 “Previous research conducted at the Manila Observatory (MO) in Quezon City, Metro Manila  
147 characterized  $\text{PM}_{2.5}$  (particulate matter (PM) with aerodynamic diameter less than  $2.5 \mu\text{m}$ ) and  
148 sources of measured particles, with traffic emissions being the major source at MO (Simpas et  
149 al., 2014). Interestingly, levels of measured  $\text{PM}_{2.5}$  at MO showed little variance between the wet  
150 (June-October) and dry seasons (Simpas et al., 2014).”

151  
152 Second, the title indicates the long-range transport mechanism will be discussed, but in the  
153 manuscript really only describes the influence of long-range transport in Quezon City. Please  
154 consider rephrase the title or include more discussion of the transport mechanism.

155  
156 Response: While our in situ ground-based measurements were taken in Quezon City, we believe  
157 that other datasets and discussions included in the manuscript broaden the scope of the transport  
158 beyond just Quezon City. For example, we include NAAPS model results at the larger scale and  
159 the discussions in Section 3.1 include descriptions of smoke transport from the maritime  
160 continent and transport of emissions from continental Asia during the typhoon.

161  
162 Following are some detailed comments.

163 Detailed comments: (1). The “abstract” section was poorly organized, and it contained too many  
164 details about method and dataset while the innovative findings and conclusions were described in  
165 a style too general for scientific publication. It begins with a very clear statement of the research  
166 objective, as “analyzes mechanisms of long-range transport and chemical characteristics”, but is  
167 followed by various types of information piece by piece. For example, line#28-29, what is the  
168 long-range transport mechanism found through this study? Is it driven by synoptic weather event,  
169 or large scale jet, or other typical or abnormal conditions? Line#30-31, the impacts of continental  
170 EA transport was identified, so what are they? Please reorganize the whole section.

171  
172 Response: We have attempted to address the specific points mentioned by the reviewer.  
173 However, we have tried to write the abstract in as straightforward a manner as possible, so we  
174 are unclear of the best method to reorganize the current form of the abstract. The revised abstract  
175 is provided here:

176  
177 “This study analyzes mechanisms of long-range transport of aerosol and aerosol chemical  
178 characteristics in and around East and Southeast Asia. Ground-based size-resolved aerosol  
179 measurements collected at the Manila Observatory in Metro Manila, Philippines from July -  
180 October 2018 were used to identify and contrast high and low aerosol loading events. Multiple  
181 data sources, including models, remote-sensing, and in situ measurements, are used to analyze  
182 the impacts of long-range aerosol transport on Metro Manila and the conditions at the local and

183 synoptic scales facilitating this transport. Through the use of case studies, evidence of long-range  
184 transport of biomass burning aerosol and continental emissions is identified in Metro Manila.  
185 Long-range transport of biomass burning aerosol from the Maritime Continent, bolstered by  
186 southwesterly flow and permitted by low rainfall, was identified through model results and the  
187 presence of biomass burning tracers (e.g. K, Rb) in the ground-based measurements. The  
188 impacts of emissions transported from continental East Asia on the aerosol characteristics in  
189 Metro Manila are also identified; for one of the events analyzed, this transport was facilitated by  
190 the nearby passage of a typhoon. Changes in the aerosol size distributions, water-soluble  
191 chemical composition, and contributions of various organic aerosol species to the total water-  
192 soluble organic aerosol were examined for the different cases. The events impacted by biomass  
193 burning transport had the overall highest concentration of water-soluble organic acids, while the  
194 events impacted by long-range transport from continental East Asia, showed high percent  
195 contributions from shorter chain dicarboxylic acids (i.e. oxalate) that are often representative of  
196 photochemical and aqueous processing in the atmosphere. The low aerosol loading event was  
197 subject to a larger precipitation accumulation than the high aerosol events, indicative of wet  
198 scavenging as an aerosol sink in the study region. This low aerosol event was characterized by a  
199 larger relative contribution from supermicrometer aerosols and had a higher percent contribution  
200 from longer-chain dicarboxylic acids (i.e. maleate) to the water-soluble organic aerosol fraction,  
201 indicating the importance of both primary aerosol emissions and local emissions. Results of this  
202 study have implications for better understanding of the transport and chemical characteristics of  
203 aerosol in a highly-populated region that has thus far been difficult to measure through remote-  
204 sensing methods. Furthermore, findings associated with the effects of air mass mixing on aerosol  
205 physiochemical properties are applicable to other global regions impacted by both natural and  
206 anthropogenic sources.”

207  
208 (2) Line#58-60: this sentence is confusing, do you want to distinguish long-range transport from  
209 synoptic scale transport?

210  
211 Response: In this sentence, we try to highlight that long-range aerosol transport occurs all over  
212 the world, yet the conditions and types of aerosols vary by region due to various factors,  
213 including regional conditions. We have re-written the sentence as follows:

214  
215 “Although impacts and processes of long-range aerosol transport have worldwide applicability,  
216 the variety of meteorological conditions and emission sources that can contribute to aerosol  
217 transport necessitate detailed analyses of transport events at the regional level.”

218  
219 (3) Line#61: there are many these kind of general common sense statements that are not really  
220 helpful in this manuscript, please consider exclude them.

221  
222 Response: We have re-written lines 61-62 to address this comment and the following comment  
223 #4:

224  
225 “The plethora of both natural and anthropogenic emissions in and around the Southeast (SE)  
226 Asia, the proximity of islands and continental regions in SE and East Asia, and the large,  
227 growing population makes SE Asia a prime candidate for the study of long-range transport of  
228 atmospheric aerosol.”

229  
230  
231  
232  
233  
234  
235  
236  
237  
238  
239  
240  
241  
242  
243  
244  
245  
246  
247  
248  
249  
250  
251  
252  
253  
254  
255  
256  
257  
258  
259  
260  
261  
262  
263  
264  
265  
266  
267  
268  
269  
270  
271  
272  
273

(4) Line#62: I didn't see any reason for starting with "however"

Response: See response above to comment #3.

(5) Line#70: "urban mega-cities" emission? Do you mean residential emission?

Response: While residential emissions are one factor in the emissions from urban mega-cities, as stated in Reid et al. (2013), differences in emissions amongst cities arise from a variety of factors, such as traffic, cooking, heating, industrial activity, etc.

(6) Line#82-86: These sentences commented the satellite-derived biomass burning emission inventory was underestimated, so the readers would expect to see further discussion about the underestimation, or how to improve it. But line#87-94 started to claim that transport mechanism of biomass burning is important. I didn't see any logistic connection between these two sections. As the importance of this study is described in line#87-94, line#82-86 is not helpful to demonstrate this importance.

Response: We believe that this description is applicable in that ground-based measurements and verifications of biomass burning can help explain and better account for the under-estimation, including both amount and frequency, of satellite-derived biomass burning emissions in the region. We have clarified this by amending the text as follows:

"In order to better understand the frequency, amount, and fate of biomass burning emissions in the MC and SE Asia, both in situ measurements and modeling studies are needed."

(7) Line#119: when is the northeast monsoon season?

Response: While variability exists in the start dates of the different seasons, Cruz et al. (2013) indicate that the transition to the northeast monsoon generally occurs in October. Bagtasa (2011) defined the northeast monsoon season from October – February. We have clarified this in the introduction by adding the following text:

"While variability exists in the start dates of the different seasons, the northeast monsoon transition generally occurs in October (Cruz et al., 2013), and previous research has defined this season as occurring from October – February (Bagtasa, 2011)."

Bagtasa, G.: Effect of Synoptic Scale Weather Disturbance to Philippine Transboundary Oxone Pollution using WRF-CHEM. Int. J. Environ. Sci. Dev., 2, 402-405, 10.7763/IJESD.2011.V2.159, 2011.

(8) Line#110-111: varies by season: smoke in Aug-Oct, dust in Feb-Apr, SWM for Jun-Sep, what about the other months? These introductions are important to justify your studying period Jul-Oct 2018 mentioned at line#138-139.

274 Response: The full sentence that the reviewer cites reads: “Another study of the aerosol over the  
275 South China Sea (SCS), which is bordered to the east by the Philippines, found seasonal changes  
276 in aerosol emission sources, with year-round anthropogenic pollution, smoke from the MC  
277 between August – October, and dust from northern continental Asia between February – April  
278 (Lin et al., 2007).” As stated, “year-round anthropogenic pollution” was measured; therefore, we  
279 believe that the other months are already addressed. Furthermore, the other studies cited discuss  
280 additional sampling periods from previous studies, biomass burning during the SWM, and  
281 aerosol from East Asia during the northeast monsoon. Therefore, we do not feel as though text  
282 revisions are needed in the draft to address this comment.

283  
284 (9) Line#139-150: I like the way that objectives and aims are clearly listed, please consider  
285 reorganize the manuscript in such a straightforward manner.

286  
287 Response: Our organization of the manuscript attempts to follow the same order in which the  
288 objectives are listed in these lines. In the results section, we begin by discussing the atmospheric  
289 conditions for each case study (objective i), followed by discussions of the composition of the  
290 size-resolved aerosol samples (objective ii). Within this discussion, we have added descriptions  
291 of transformational processes that we observe, especially with regards to the organic aerosol  
292 (objective iii). Therefore, we believe that the organization of the manuscript already mirrors that  
293 of the objectives.

294  
295 (10) Line#141: Confusing, please rephrase this sentence: isolate characteristic aerosol  
296 physicochemical properties indicative of long-range transport

297  
298 Response: We have re-worded as follows:

299  
300 “(ii) characterize aerosol physicochemical properties associated with long-range transport.”

301  
302 (11) Table1: please explain why the sampling period was 2-day, and why the starting time was  
303 different, some in the morning and some in the afternoon

304  
305 Response: We received a very similar comment from Referee #1 and have listed our response to  
306 their comment here:

307  
308 “The initial sets were taken at the very beginning of a year-long sampling campaign. As these  
309 measurements were new to the metro Manila environment, we were unclear of how long to run  
310 the instrumentation for optimal sampling. Therefore, the variations in sample lengths represent  
311 different tests until we settled on a 2-day sampling window. However, for all sets, we attempted  
312 to sample in increments of 24 hrs in order to minimize diurnal influences. Furthermore, the  
313 length of sampling factors into the conversion of the aqueous concentrations to air-equivalent  
314 measurements. Therefore, we believe any differences in measurements due to varying sampling  
315 windows are minimized. We do not feel as though text revisions are needed in the draft to  
316 address this comment.”

317  
318 (12) Line#245: water-soluble aerosol refers to the species shown in Fig.6? are these  
319 measurements for ambient air concentrations?



320  
321  
322  
323  
324  
325  
326  
327  
328  
329  
330  
331  
332  
333  
334  
335  
336  
337  
338  
339  
340  
341  
342  
343  
344  
345  
346  
347  
348  
349  
350  
351  
352  
353  
354  
355  
356  
357

Response: Our method for analyzing the chemical composition of the ambient aerosol was to extract the filter samples in water. Therefore, all concentrations described are for the water-soluble component of the aerosol only.

(13) Fig.2: why there are multiple blue lines for back-trajectories, did you trace back at different altitude?

Response: As stated in the methodology section, “The model was run for back-trajectories terminating at the MOUDI inlet (~85 m above sea level) every 6 h during each sample set.” This results in multiple back-trajectories for each sample set, since each set was run for at least 24 hrs, with most run for 48 hrs. We have clarified this by amending the text as follows:

“The model was run for back-trajectories terminating at the MOUDI inlet (~85 m above sea level) starting at the beginning of the sample set and every 6 h thereafter during each sample set, resulting in  $(1 + N/6)$  trajectories for each set, where N is the total number of sampling hours.”

(14) Line255-257: the NAAPS only shows the surface concentration, the MC smoke may not necessarily transport all the way to Quezon, this is why the altitude of HYSPLIT also need to be demonstrated to correlate the source and receptor

Response: As stated in the methodology section, “The model was run for back-trajectories terminating at the MOUDI inlet (~85 m above sea level).” Since we were trying to correlate our surface measurements with the transport patterns, we wanted to use only HYSPLIT back-trajectories that ended at our surface site altitude. While we ran the HYSPLIT model for this altitude only, we believe that this is representative of the region, due to a previous work that has shown the significance of boundary layer transport in the region. Furthermore, as shown in the CALIPSO overpasses, it appears that the aerosol layer extends from the surface.

(15) Section3.2.3: the concentration of organic aerosol seems very low, can you show the total ambient air concentration of OA, other than the water-soluble aerosol?

Response: Unfortunately, we do not have concentrations of the water insoluble components. However, as shown in the analysis by Cruz et al. (2019), black carbon measurements were conducted for one sample set and the filters were weighed for two other sets. The results show that there are significant fractions of black carbon and unresolved aerosol mass, which could be insoluble organic and inorganic components.

1 Long-Range Transport Mechanisms in East and Southeast Asia and Impacts on Size-Resolved  
2 Aerosol Composition: Contrasting High and Low Aerosol Loading Events  
3  
4

5 Rachel A. Braun<sup>1</sup>, Mojtaba Azadi Aghdam<sup>1</sup>, Paola Angela Bañaga<sup>2,3</sup>, Grace Betito<sup>3</sup>, Maria  
6 Obiminda Cambaliza<sup>2,3</sup>, Melliza Templonuevo Cruz<sup>2,4</sup>, Genevieve Rose Lorenzo<sup>2</sup>, Alexander B.  
7 MacDonald<sup>1</sup>, James Bernard Simpas<sup>2,3</sup>, Connor Stahl<sup>1</sup>, Armin Sorooshian<sup>1,5</sup>  
8  
9

10 <sup>1</sup>Department of Chemical and Environmental Engineering, University of Arizona, Tucson, AZ,  
11 USA

12 <sup>2</sup>Manila Observatory, Loyola Heights, Quezon City 1108, Philippines

13 <sup>3</sup>Department of Physics, School of Science and Engineering, Ateneo de Manila University,  
14 Loyola Heights, Quezon City 1108, Philippines

15 <sup>4</sup>Institute of Environmental Science and Meteorology, University of the Philippines, Diliman,  
16 Quezon City 1101, Philippines

17 <sup>5</sup>Department of Hydrology and Atmospheric Sciences, University of Arizona, Tucson, AZ, USA  
18

19 Correspondence to: Armin Sorooshian (armin@email.arizona.edu)

20 **Abstract**

21 This study analyzes mechanisms of long-range transport of aerosol and aerosol chemical  
22 characteristics in and around East and Southeast Asia. Ground-based size-resolved aerosol  
23 measurements collected at the Manila Observatory in Metro Manila, Philippines from July -  
24 October 2018 were used to identify and contrast high and low aerosol loading events. Multiple  
25 data sources, including models, remote-sensing, and in situ measurements, are used to analyze  
26 the impacts of long-range aerosol transport on Metro Manila and the conditions at the local and  
27 synoptic scales facilitating this transport. Evidence Through the use of case studies, evidence of  
28 long-range transport of biomass burning aerosol and continental emissions is identified in Metro  
29 Manila.  
30 Long-range transport of biomass burning aerosol from the Maritime Continent, bolstered by  
31 southwesterly flow and permitted by low rainfall, was identified through model results and the  
32 presence of biomass burning tracers (e.g. K, Rb) in the ground-based measurements. The  
33 impacts of emissions transported from continental East Asia on the aerosol characteristics in  
34 Metro Manila are also identified; for one of the events analyzed, this transport was facilitated by  
35 the nearby passage of a typhoon. Changes in the aerosol size distributions, water-soluble  
36 chemical composition, and contributions of various organic aerosol species to the total water-  
37 soluble organic aerosol were examined for the different cases. The events impacted by biomass  
38 burning transport had the overall highest concentration of water-soluble organic acids, while the  
39 events impacted by long-range transport from continental East Asia, showed high percent  
40 contributions from shorter chain dicarboxylic acids (i.e. oxalate) that are often representative of  
41 photochemical and aqueous processing in the atmosphere. The low aerosol loading event was  
42 subject to a larger precipitation accumulation than the high aerosol events, indicative of wet  
43 scavenging as an aerosol sink in the study region. This low aerosol event was characterized by a  
44 larger relative contribution from supermicrometer aerosols and had a higher percent contribution  
45 from longer-chain dicarboxylic acids (i.e. maleate) to the water-soluble organic aerosol fraction,  
46 indicating the importance of both primary aerosol emissions and local emissions. Results of this  
47 study have implications for better understanding of the transport and chemical characteristics of  
48 aerosol in a highly-populated region that has thus far been difficult to measure through remote-  
49 sensing methods. Furthermore, findings associated with the effects of air mass mixing on aerosol  
50 physiochemical properties are applicable to other global regions impacted by both natural and  
51 anthropogenic sources.

52

## 53 1. Introduction

54 Better understanding of long-range transport of aerosol is critical for determining the fate  
55 of atmospheric emissions and improving models of atmospheric aerosol. Nutrients (e.g. Duce et  
56 al., 1991; Artaxo et al., 1994), bacteria (e.g. Bovallius et al., 1978; Maki et al., 2019), and  
57 pollutants (e.g. Nordø, 1976; Lyons et al., 1978; Lindqvist et al., 1991) can be transported  
58 through the atmosphere over large distances across the globe. Atmospheric aerosol can undergo  
59 physiochemical changes through photochemical and aqueous-processing mechanisms such that  
60 their characteristics at the emission source can be quite different from those farther downwind  
61 (e.g. Yokelson et al., 2009; Akagi et al., 2012). Large uncertainties remain in atmospheric  
62 aerosol models due to impacts of aqueous processing and wet scavenging on aerosol (Kristiansen  
63 et al., 2016; Xu et al., 2019). Although impacts and processes of long-range aerosol transport  
64 have worldwide applicability, the ~~strong facilitation~~ variety of transport by synoptic  
65 sea level meteorological conditions ~~neecessitates~~ and emission sources that can contribute to aerosol  
66 transport necessitate detailed analyses of transport events at the regional level.

67 ~~Both The plethora of both~~ natural and anthropogenic emissions ~~contribute to atmospheric~~  
68 ~~aerosol worldwide. However, the plethora of both types of sourees~~ in and around the Southeast  
69 (SE) Asia, the proximity of islands and continental regions in SE and East Asia, and the large,  
70 growing population makes SE Asia a prime candidate for the study of long-range transport of  
71 atmospheric aerosol. Moreover, the extensive cloud coverage and precipitation during certain  
72 times of the year in SE Asia allow for an examination of the effects of aqueous processing and  
73 wet scavenging. Characterizations of aerosol in mainland SE Asia and the Maritime Continent  
74 (MC), which includes the islands south of the Philippines and north of Australia (e.g. islands part  
75 of Malaysia and Indonesia), have found major emission sources to be industrial activities,  
76 shipping, urban mega-cities, and biomass burning (Reid et al., 2013). In addition, natural  
77 emission sources, including marine emissions, plant life, and occasionally volcanic eruptions,  
78 intermingle with anthropogenic emissions. Mixing of aerosol from anthropogenic and biogenic  
79 sources has been noted to be influential in the overall production of secondarily produced aerosol  
80 via gas-to-particle conversion processes (Weber et al., 2007; Goldstein et al., 2009; Brito et al.,  
81 2018). In addition, the mixing of marine and biomass burning emissions can produce  
82 compositional changes, such as enhancements in chloride depletion (e.g. Braun et al., 2017) and  
83 methanesulfonate (MSA) production (Sorooshian et al., 2015). The mechanisms governing  
84 aerosol changes in mixed air masses have wide-ranging and complex impacts and require further  
85 study in regions, such as SE Asia, that are impacted by multiple aerosol emission sources.

86 One major contributor to atmospheric aerosol in SE Asia and the MC that has received  
87 considerable attention is biomass burning. Biomass burning in SE Asia appears to be dominated  
88 by anthropogenic activities, such as peatland burning (Graf et al., 2009; Reid et al., 2013; Latif et  
89 al., 2018) and rice straw open field burning (Gadde et al., 2009). However, current satellite  
90 retrievals underestimate the true emissions in the region (Reid et al., 2013). Identification of  
91 biomass burning emissions in the MC using satellite-based observations is difficult for numerous  
92 reasons, including the characteristics of fires common to the region (e.g. low-temperature peat-  
93 burning) and abundant cloud cover (Reid et al., 2012, 2013). However, the potential for long-  
94 range transport of biomass burning emissions from the MC has received considerable attention  
95 (Wang et al., 2013; Xian et al., 2013; Reid et al., 2016a; Atwood et al., 2017; Ge et al., 2017;  
96 Song et al., 2018). In order to better understand the prevalence frequency, amount, and fate of  
97 biomass burning emissions in the MC and SE Asia, both in situ measurements and modeling  
98 studies are needed. Insights into the fate of biomass burning emissions in the atmosphere are

99 crucial and applicable on a global scale, especially since studies have indicated an increasing  
100 trend in biomass burning worldwide (Flannigan et al., 2009, 2013).

101 As a mega-city in SE Asia, Metro Manila, Philippines (Population ~12.88 million;  
102 Philippine Statistics Authority, 2015) is a prime location for the study of locally-produced urban  
103 anthropogenic aerosol (Kim Oanh et al., 2006) that is mixed with biogenic, natural, and  
104 anthropogenic pollutants from upwind areas. Previous research conducted at the Manila  
105 Observatory (MO) in Quezon City, Metro Manila characterized ~~seasonal trends in~~ PM<sub>2.5</sub>  
106 (particulate matter (PM) with aerodynamic diameter less than 2.5 μm) and sources of measured  
107 particles, with traffic emissions being the major source at MO (Simpas et al., 2014).

108 Interestingly, levels of measured PM<sub>2.5</sub> at MO showed little variance between the wet (June-  
109 October) and dry seasons (Simpas et al., 2014). Additional studies have further characterized  
110 vehicular emissions by focusing on black carbon (BC) particulate concentrations in sites around  
111 the Metro Manila region, including near roadways (Bautista et al., 2014; Kecorius et al., 2017;  
112 Alas et al., 2018). Due to very high population density in Metro Manila, it is expected that many  
113 of the urban PM sampling sites are highly affected by local anthropogenic sources as opposed to  
114 long-range transport. However, the proximity of the Philippines to other islands and continental  
115 Asia raises the question of the relative impacts of long-range transport as opposed to local  
116 emissions on not just Metro Manila, but also downwind regions.

117 Long-range transport to the Philippines varies by season since there is a strong change in  
118 weather patterns throughout the year (Bagtasa et al., 2018). Another study of the aerosol over the  
119 South China Sea (SCS), which is bordered to the east by the Philippines, found seasonal changes  
120 in aerosol emission sources, with year-round anthropogenic pollution, smoke from the MC  
121 between August – October, and dust from northern continental Asia between February – April  
122 (Lin et al., 2007). The season from approximately June – September (Cayanan et al., 2011; Cruz  
123 et al., 2013), referred to as the Southwest Monsoon (SWM) season, is characterized by increased  
124 prevalence of southwesterly winds and precipitation. During the SWM season, biomass burning  
125 is prevalent in the MC, while biomass burning is more common in continental SE Asia during  
126 the winter and spring (Lin et al., 2009; Reid et al., 2013). While variability exists in the start dates  
127 of the different seasons, the northeast monsoon transition generally occurs in October (Cruz et  
128 al., 2013), and previous research has defined this season as occurring from October – February  
129 (Bagtasa, 2011). During the northeast monsoon, aerosol influences from northern East Asia were  
130 measured in the northwestern edge of the Philippines (Bagtasa et al., 2018). In addition to  
131 transport of aerosol to the Philippines, the influence of emission outflows from the Philippines  
132 has also been measured in the northern SCS at Dongsha Island (Chuang et al., 2013) and in  
133 coastal southeast China (Zhang et al., 2012). Long-range transported aerosol in SE and East Asia  
134 have various sources, and therefore, different physiochemical properties. However, the  
135 prevalence of the signal of long-range transported aerosol in a highly polluted mega-city, such as  
136 Metro Manila, is not well characterized.

137 As recent studies have indicated a decline in SWM rainfall in the western Philippines and  
138 an increase in no-rain days during the typical SWM season (Cruz et al., 2013), the potential for  
139 wet scavenging of aerosol during these time periods could be decreasing. Furthermore, decreases  
140 in monsoonal rainfall in other parts of Asia, including India (Dave et al., 2017) and China (Liu et  
141 al., 2019), have been linked to increases in aerosol, especially those of anthropogenic origin.  
142 Reinforcing mechanisms in these interactions, such as decreased rainfall reducing wet  
143 scavenging, leading to higher aerosol concentrations that in turn suppress precipitation, and the  
144 corresponding climatic changes in monsoonal rain in the western Philippines underscore the need

145 to better understand the processes governing atmospheric aerosol characteristics and sources,  
146 especially during the monsoonal season.

147 The present study focuses on three high-aerosol loading events, contrasted with a very  
148 low aerosol event, as identified by ground-based observations collected at MO from July -  
149 October 2018. The objectives of the study are to (i) describe synoptic and local scale conditions  
150 facilitating various transport cases, (ii) ~~isolate characteristic~~ characterize aerosol  
151 ~~physiochemical~~ physicochemical properties ~~indicative of~~ associated with long-range transport, and  
152 (iii) identify transformational processes, especially with regard to chemical composition, of  
153 aerosol during long-range transport to the highly-populated Metro Manila region. The results of  
154 this work have implications for better understanding of (i) the fate of biomass burning emissions  
155 in a region with prevalent wildfires that are poorly characterized by remote-sensing, (ii) the  
156 impact of transformational and removal mechanisms, including aqueous processing,  
157 photochemical reactions, and wet scavenging, on long-range transported aerosol from multiple  
158 sources, and (iii) typical synoptic and local scale behavior of aerosol in a region that is both  
159 highly populated and gaining increasing attention due to campaigns such as the NASA-  
160 sponsored Clouds, Aerosols, and Monsoon Processes Philippines Experiment (CAMP<sup>2</sup>Ex).

## 161 **2. Methodology**

### 162 **2.1 Ground-Based Observations**

163 As part of a year-long sampling campaign (CAMP<sup>2</sup>Ex weathER and CompoSition  
164 Monitoring: CHECSM) at the Manila Observatory (MO; 14.64° N, 121.08° E) in Quezon City,  
165 Metro Manila, Philippines, 12 sets of size-resolved aerosol were collected from July - October  
166 2018 using a Micro-Orifice Uniform Deposit Impactor (MOUDI; Marple et al., 2014). Details  
167 for the 12 size-resolved sets can be found in Table 1. Sample Teflon substrates (PTFE  
168 membrane, 2 μm pore, 46.2 mm diameter, Whatman) were cut in half for preservation for future  
169 analysis. Half-substrates were extracted in 8 mL of Milli-Q water (18.2 MΩ-cm) in sealed  
170 polypropylene vials through sonication for 30 min. Aqueous extracts were subsequently analyzed  
171 for ions using ion chromatography (IC; Thermo Scientific Dionex ICS-2100 system) and  
172 elements using triple quadrupole inductively coupled plasma mass spectrometry (ICP-QQQ;  
173 Agilent 8800 Series). The list of analyzed species and limits of detection for those species can be  
174 found in Table S1, with limits of detection in the ppt range for ICP and the ppb range for IC.  
175 Background concentrations were also subtracted from each sample. For each MOUDI set  
176 (naming convention: MO#), the mass concentration sum of the water-soluble species was  
177 calculated; using this summation, the three high-aerosol loading events were identified (MO7,  
178 MO12, and MO14), as well as the lowest aerosol event (MO11). The average ± standard  
179 deviation of the total-water soluble species measured for the remaining 8 sets not identified in  
180 the high or low categories is  $6.99 \pm 2.71 \mu\text{g m}^{-3}$ .

### 181 **2.2 Remote-Sensing Observations**

182  
183 Retrievals of atmospheric profiles from the Cloud-Aerosol Lidar with Orthogonal  
184 Polarization (CALIOP) onboard the Cloud-Aerosol Lidar and Infrared Pathfinder Satellite  
185 Observations (CALIPSO) were taken for select satellite overpasses corresponding to MOUDI  
186 sample sets of interest (Winker et al., 2009). Previous studies have examined the ability of  
187 CALIOP to capture atmospheric profiles in SE Asia and the MC, with one major challenge in  
188 this region being the lack of cloud-free schemes (Campbell et al., 2013; Ross et al., 2018).  
189 Overpasses corresponding to the three highest aerosol events were analyzed, but no data was  
190

191 available for the time encompassing MO11. The CALIOP Level 2 Vertical Feature Mask (VFM)  
192 [Version 4.20](#) was used to distinguish between clear air, clouds, and aerosol (Vaughan et al.,  
193 2004). [For figures of CALIOP VFM data in this study, data are plotted at 30 m vertical](#)  
194 [resolution every 5 km along the satellite ground-track.](#)

## 196 2.3 Models

197 To describe the synoptic scale conditions, data were used from the Modern-Era  
198 Retrospective analysis for Research and Applications, Version 2 (MERRA-2; Gelaro et al.,  
199 2017). Horizontal winds at 850 hPa (GMAO, 2015a) were temporally averaged over the  
200 sampling period using 3-hourly instantaneous data and subsequently spatially averaged to  
201 increase figure readability. The total cloud area fraction (GMAO, 2015b) was also temporally  
202 averaged over the sampling period using 1-hourly time-averaged MERRA-2 data.

203 Five-day air mass back-trajectories were calculated using the Hybrid Single Particle  
204 Lagrangian Integrated Trajectory (HYSPLIT) model from NOAA (Stein et al., 2015) and  
205 gridded meteorological data from the National Centers for Environmental Prediction/National  
206 Center for Atmospheric Research (NCEP/NCAR) reanalysis project. The model was run for  
207 back-trajectories terminating at the MOUDI inlet (~85 m above sea level) [starting at the](#)  
208 [beginning of the sample set and](#) every 6 h [thereafter](#) during each sample set, [resulting in \(1 +](#)  
209 [N/6\) trajectories for each set, where N is the total number of sampling hours.](#) The HYSPLIT  
210 model has been used extensively in studies focused on regions across the globe to study aerosol  
211 transport (Stein et al., 2015).

212 Precipitation amounts were found using the Precipitation Estimation from Remotely  
213 Sensed Information using Artificial Neural Networks—Cloud Classification System  
214 (PERSIANN-CCS) dataset (Hong et al., 2004), which is available from the UC Irvine Center for  
215 Hydrometeorology and Remote Sensing (CHRS) Data Portal (<http://chrsdata.eng.uci.edu>,  
216 Nguyen et al., 2019). PERSIANN-CCS has previously been used to analyze precipitation events  
217 in the region of interest, as shown by the successful characterization of rainfall during Typhoon  
218 Haiyan over the Philippines in November 2013 (Nguyen et al., [2014](#)). [Benefits of PERSIANN-](#)  
219 [CCS include the data availability at 0.04° x 0.04° spatial resolution, while uncertainties in the](#)  
220 [dataset arise from sources such as a lack of bias correction \(Nguyen et al., 2014\).](#) Precipitation  
221 accumulated during the sample sets (Table 1) was calculated to be the average found for the  
222 region surrounding MO in the box bounded by 121.0199 - 121.0968° E and 14.6067 - 14.6946°  
223 N.

224 To further describe long-range transport activity, results from the Navy Aerosol Analysis  
225 and Prediction System (NAAPS) operational model are included for the selected study periods  
226 (Lynch et al., 2016; <https://www.nrlmry.navy.mil/aerosol/>). Global meteorological fields used in the  
227 NAAPS model are supplied by the Navy Global Environmental Model (NAVEM; Hogan et al.,  
228 2014). The NAAPS model has previously been employed to study aerosol in the MC (e.g. Xian  
229 et al., 2013).

## 231 3. Results

### 232 3.1 Cases of Long-Range Aerosol Transport

233 The following sub-sections (3.1.1-3.1.4) describe the synoptic and local scale  
234 meteorological conditions governing long-range aerosol transport during the three highest  
235 aerosol events (MO7, MO12, and MO14) and, for the purposes of comparison, the lowest aerosol

236 event (MO11). Also included are characterizations of aerosol from remote-sensing and model  
237 results. Results of size-resolved aerosol characterization at MO are discussed in Section 3.2.  
238

### 239 **3.1.1 MO7 (August 14 – 16, 2018): Smoke Transport from Maritime Continent**

240 Many previous studies have focused on the prevalence of biomass burning in the MC and  
241 the potential for transport of smoke towards the Philippines (Wang et al., 2013; Xian et al., 2013;  
242 Reid et al., 2016a; Atwood et al., 2017; Ge et al., 2017; Song et al., 2018). Figure 1a shows the  
243 average 850 hPa wind vectors and cloud fraction for the MO7 sampling period. The prevailing  
244 wind direction was towards the northeast, consistent with typical SWM flow. Furthermore, areas  
245 with lower cloud coverage were present to the southwest of Metro Manila. The HYSPLIT back-  
246 trajectory for this sample set also shows an air mass originating around the MC to the southwest  
247 of MO that is then transported over the ocean towards the Philippines (Figure 2a). As evidenced  
248 by the name of the season (i.e. Southwest Monsoon), this trajectory is typical for this time of the  
249 year and was the dominating trajectory pattern for the remaining eight sample sets not chosen for  
250 in-depth analysis (Figure S1). Furthermore, for MO1 – MO10 (i.e. all sample sets with prevailing  
251 southwesterly wind influence), MO7 had the lowest rain amount for the surrounding region,  
252 followed by MO8, which had the 4<sup>th</sup> highest water-soluble aerosol concentration (Table 1). This  
253 suggests that wet scavenging could have been less influential in MO7 and MO8, thereby leading  
254 to an increase in the PM measured. Three CALIPSO overpasses near MO occurred during the  
255 MO7 sample set and one occurred during the nighttime after sampling ended; however, the  
256 signal was largely attenuated in the lower 8 km during the daytime samples for the area  
257 surrounding MO (Figure S2). In the case of the two nighttime overpasses (Figure 3), which  
258 sampled to the southwest of Manila, a deep aerosol layer is observed in the VFM extending from  
259 the surface to around 3 km (Figure 3). This classic case of long-range transport from the MC to  
260 the Philippines during the SWM season is also clearly shown in the biomass burning smoke  
261 surface concentrations from the NAAPS model (Figure 4a).  
262

### 263 **3.1.2 MO11 (September 18 – 20, 2018): Lowest Aerosol Event**

264 MO11 had the lowest overall water-soluble aerosol mass concentration ( $2.7 \mu\text{g m}^{-3}$ ),  
265 which is over six times lower than the highest aerosol MOUDI set. As evidenced by both the 850  
266 hPa wind vectors (Figure 1b) and the HYSPLIT back-trajectories (Figure 2b) from this set,  
267 conditions are very different from the highest three aerosol events and show transport patterns  
268 with flow originating over the open ocean to the east of the Philippines moving almost due west.  
269 The lack of anthropogenic aerosol sources in the path of the back-trajectories could result in the  
270 overall low amount of aerosol observed. This set was also characterized by high accumulated  
271 rainfall amounts for the region in the path of the back-trajectories (Figure 2b) and in the area  
272 surrounding MO as compared to the highest aerosol events (Table 1), increasing the possibility  
273 that wet scavenging effectively removed most of the transported (and, to some extent, local)  
274 aerosol. In addition, the NAAPS model showed no smoke influence from the MC and an isolated  
275 anthropogenic and biogenic fine aerosol plume around Metro Manila, suggesting local sources  
276 accounted for the majority of the measured aerosol (Figure 4b).  
277

### 278 **3.1.3 MO12 (September 26 – 28, 2018): Impacts of Typhoon Trami**

279 Typhoon Trami (Category 5) passed to the northeast of the island of Luzon in the  
280 Philippines during MO12 (Figure 1c). Typhoon influences on atmospheric aerosol, caused by  
281 varying factors such as wind speed and precipitation, have been studied in China (Yan et al.,



282 2016; Liu et al., 2018), Korea (Kim et al., 2007), Malaysia (Juneng et al., 2011), the South China  
283 Sea (Reid et al., 2015, 2016b), and Taiwan (Fang et al., 2009; Chang et al., 2011; Lu et al.,  
284 2017). The influences of typhoons on biomass burning emissions and transport in the MC have  
285 also been examined (Reid et al., 2012; Wang et al., 2013). In this case, the influence of this storm  
286 changed the prevailing wind direction approaching the northern Philippines, effectively pulling  
287 an air mass from the west of the island, and along with it, emissions from continental East Asia  
288 (Figure 2c). Furthermore, the air mass passed through regions of relatively little rainfall during  
289 transport to the Philippines (Figure 2c), and accumulated rainfall at MO during this sample set  
290 was very low (Table 1). One CALIPSO overpass around the ending time of set MO12 and one  
291 during the nighttime after sampling ended (Figure 3) show that in the direction of transport (i.e.  
292 north of the MO, from around 15-20° N), there is an aerosol layer extending up to around 2 km  
293 during the day (northwest of MO) and 3 km at night (northeast of MO). The influence of  
294 emissions from continental East Asia is also apparent in the NAAPS model (Figure 4c).  
295 Observations at Dongsha Island, located to the north of the Philippines, have revealed influence  
296 from Gobi Desert emissions (Wang et al., 2011) and anthropogenic sources (Atwood et al.,  
297 2013). Farther south in the MC, aerosol measurements in Malaysia have also indicated influence  
298 of aged, long-range transport from sites to the north in East Asia (Farren et al., 2019).  
299

### 300 **3.1.4 MO14 (October 6 – 8, 2018): Mixed Influences**

301 The final MOUDI set (MO14) included in this study represents a transition in  
302 meteorological regimes at the end of the SWM season and resulted in the highest overall water-  
303 soluble mass concentration. This event had some of the lowest rainfall amounts in the region  
304 surrounding Metro Manila (Figure 2d), with zero accumulated precipitation at MO during the  
305 sampling period (Table 1). Furthermore, low cloud fraction was observed for regions to the  
306 northwest and east of Metro Manila (Figure 1d). Back-trajectories from HYSPLIT show that the  
307 air mass appeared to be influenced by a mix of continental sources in East Asia and local sources  
308 (Figure 2d). Furthermore, two CALIPSO overpasses, one during the nighttime while sampling  
309 was occurring and the other during the daytime after sampling ended, show a deep aerosol layer  
310 north of MO, extending from the surface to around 2 km on October 6<sup>th</sup> and lower on October 8<sup>th</sup>  
311 (Figure 3). From the NAAPS model, it appears that a mixture of MC smoke emissions and  
312 continental East Asia emissions converge around the northern Philippines (Figure 4d).  
313

## 314 **3.2. Ground-Based Aerosol Chemical Composition**

### 315 **3.2.1 Size-Resolved Aerosol Characteristics**

316 The water-soluble mass size distributions and the percent contribution of each MOUDI  
317 stage to the water-soluble mass for the four sets of interest (MO7, MO12, MO14, and MO11)  
318 and the average ( $\pm$  one standard deviation) of the remaining sets (MO1 – MO6, MO8 – MO10)  
319 are shown in Figure 5. Most of the sets show a bimodal distribution with peaks in both the  
320 submicrometer and supermicrometer range; one exception is the lowest aerosol event (MO11),  
321 which shows a fairly broad size distribution. The highest aerosol event, MO14, shows a  
322 significant peak in the submicrometer range, with a very large drop in mass concentration in the  
323 supermicrometer range. This is in stark contrast to the lowest aerosol event (MO11), which  
324 shows that the supermicrometer range contributes the greatest percent to the total water-soluble  
325 mass. The second and third highest aerosol events, MO7 and MO12, also show significant  
326 enhancements in the supermicrometer range as compared to the average of the other sets and  
327 MO14.

328 Examination of the major species contributing to the water-soluble mass (Figure 6) can  
329 lend additional insights into the variability in the size distributions. MO14 had one of the highest  
330 combined contributions of  $\text{SO}_4^{2-}$  and  $\text{NH}_4^+$  (77.2% of water-soluble mass), with only MO10  
331 being slightly larger at 77.6%. These two species are typically associated with the submicrometer  
332 range and anthropogenic origins due to their formation through secondary processes such as gas-  
333 to-particle conversion of gaseous  $\text{SO}_2$  and  $\text{NH}_3$ , respectively, and aqueous processing to form  
334  $\text{SO}_4^{2-}$  (Ervens, 2015). In contrast, MO11 had the lowest overall combined percent contribution of  
335 these two species (41.4%) to the water-soluble aerosol mass. Of all 12 SWM MOUDI sets,  
336 MO11 had the highest percent contributions from  $\text{Ca}^{2+}$  (14.0%) and  $\text{Cl}^-$  (12.5%), as well as one  
337 of the highest contributions from  $\text{Na}^+$  (10.7%). Each of these species is associated with primary  
338 emissions, including dust in the case of  $\text{Ca}^{2+}$  and sea salt for  $\text{Na}^+$  and  $\text{Cl}^-$ , resulting in larger  
339 particles (i.e.  $> 1 \mu\text{m}$ ). The HYSPLIT back-trajectories for MO11 match well with the MOUDI  
340 results, as the influence of marine aerosol (i.e.  $\text{Na}^+$ ,  $\text{Cl}^-$ ) and lack of anthropogenic sources of  
341  $\text{SO}_2$  and  $\text{NH}_3$  is apparent. Local sources of dust most likely contribute the highest amount to the  
342 measured  $\text{Ca}^{2+}$ , as the back-trajectories show few other crustal sources farther upwind. Average  
343 size-resolved profiles for all of the species in these 12 sample sets can be found in Cruz et al.  
344 (2019), with characteristic size distribution profiles agreeing with the above assessments.  
345

### 346 3.2.2 Enhancements in Tracer Species

347 In addition to insights from the major water-soluble chemical species found in aerosol,  
348 tracer aerosol species can also be used to identify impacting emission sources (e.g. Fung and  
349 Wong, 1995; Allen et al., 2001; Ma et al., 2019). For the aforementioned high aerosol events,  
350 numerous tracer species are elevated in some, but not all, sample sets. This makes these species  
351 prime candidates for linking influencing sources to the measured ambient aerosol. The authors  
352 theorize that MO8, which was the 4<sup>th</sup> highest aerosol event (Table 1), also was impacted by  
353 biomass burning due to the back-trajectory analysis (Figure S1), NAAPS model (Figure S3), and  
354 increases in select species described subsequently. Therefore, MO8 was separated from the other  
355 sample sets for the purposes of the following characterizations. Figure 7 shows the size-resolved  
356 aerosol composition for select tracer species for the four highest aerosol events (MO7, MO8,  
357 MO12, and MO14), the lowest aerosol event (MO11), and the average ( $\pm$  standard deviation) of  
358 the remaining seven sample sets.

359 Potassium is frequently used as a biomass burning tracer (e.g. Andreae, 1983; Artaxo et  
360 al., 1994; Echalar et al., 1995; Chow et al., 2004; Thepnuan et al., 2019). This species shows  
361 highly elevated levels in the submicrometer range for MO7 and MO8 (i.e. the sets influenced by  
362 biomass burning transport from the MC). Other elevated trace elements for these two profiles  
363 include Rb, Cs, Se, and Ti (Figure 7). Previous studies in the western United States (Schlosser et  
364 al., 2017; Ma et al., 2019) have also shown Rb enhancements in wildfire-influenced aerosol. Rb  
365 has also been measured in flaming and smoldering biomass burning emissions (Yamasoe et al.,  
366 2000). Enhancements in Rb and Cs in the fine fraction of aerosol influenced by wildfire  
367 emissions have been observed in South Africa (Maenhaut et al., 1996), with similar results  
368 shown in this study for aerosol in the submicrometer size range. Se is also enhanced for these  
369 two sets in the submicrometer range, as it is often formed through gas-to-particle conversion  
370 processes of inorganic Se compounds (Wen and Carignan, 2007). A wide variety of sources for  
371 atmospheric Se exist (Mosher and Duce, 1987), including, but not limited to, coal combustion  
372 (Thurston and Spengler, 1985; Fung and Wong, 1995; Song et al., 2001), marine emissions  
373 (Arimoto et al., 1995), volcanos, and biomass burning (Mosher and Duce, 1987). In contrast to

374 the other enhanced species for MO7 and MO8, the mass concentration mode for Ti resides in  
375 supermicrometer size range. Ti is typically associated with crustal material that can be suspended  
376 through mechanisms such as vehicle usage (Sternbeck et al., 2002; Querol et al., 2008; Amato et  
377 al., 2009) and lofting in wildfire plumes (Maudlin et al., 2015; Schlosser et al., 2017). While  
378 long-range transport of biomass burning aerosol could lead to the enhancements measured for  
379 these biomass burning tracer species, local emission sources, such as waste burning and wood  
380 burning for cooking, may also play a role.

381 Two tracer species are included that showed enhancements for MO12, specifically Ba in  
382 the supermicrometer range and V in the submicrometer range (Figure 7). One well-documented  
383 source of aerosol Ba is non-exhaust vehicle emissions, including brakewear (Sternbeck et al.,  
384 2002; Querol et al., 2008; Amato et al., 2009; Jeong et al., 2019). V also has well characterized  
385 emission sources, most specifically fuel combustion (Fung and Wong, 1995; Artaxo et al., 1999;  
386 Song et al., 2001; Lin et al., 2005; Kim and Hopke, 2008). In coastal environments, V is often  
387 tied to shipping emissions (Agrawal et al., 2008; Pandolfi et al., 2011; Maudlin et al., 2015;  
388 Mamoudou et al., 2018). As these sources are anthropogenic in origin, it is difficult to determine  
389 the relative influences of long-range transport versus local emissions, especially with the  
390 proximity of the sampling site to major roadways and shipping in Manila Bay. However, the  
391 enhancement in V could result from the transport of the aerosol over major shipping lanes father  
392 upwind.

393 Finally, Figure 7 shows three selected elements that appear enhanced in MO14, all of  
394 which are typically tied to anthropogenic sources. Both Pb and Sn are found mainly in the  
395 submicrometer range and have been linked by previous studies to vehicle emissions (Singh et al.,  
396 2002; Amato et al., 2009), industrial emissions (Querol et al., 2008; Allen et al., 2001), and  
397 waste burning (Kumar et al., 2015). Other sources of Pb could include E-waste recycling  
398 (Fujimori et al., 2012) and biomass burning (Maenhaut et al., 1996). The size distribution of Mo  
399 for MO14 shows a much broader distribution, with peaks in both the sub- and supermicrometer  
400 ranges. Sources of Mo include vehicle emissions (Pakkanen et al., 2003; Amato et al., 2009),  
401 combustion (Pakkanen et al., 2001, 2003), and industrial activity, including copper smelters  
402 (Artaxo et al., 1999). As is the case with the enhanced species in MO12, the anthropogenic  
403 nature of these species makes it difficult to determine the relative contribution of long-range  
404 versus local emissions. However, as both MO12 and MO14 show enhancements in  
405 anthropogenic-produced trace elements, the influence of long-range transport from industrial and  
406 urban areas in continental East Asia is plausible.

407

### 408 **3.2.3 Variability of Water-Soluble Organic Species**

409 Water-soluble organic aerosol species serve as good tracers for emission sources, impact  
410 the cloud condensation nuclei (CCN) budget, and contribute non-negligible mass to atmospheric  
411 aerosol. Figure 8 shows the sum of the total measured water-soluble organic species and the  
412 relative contributions of oxalate, succinate, adipate, maleate, pyruvate, MSA, and phthalate to the  
413 total measured water-soluble organics for MO7, MO8, MO11, MO12, MO14, and the average ( $\pm$   
414 one standard deviation) of the remaining sets. Malonate (C3) was not characterized due to its low  
415 concentrations in the samples measured and the co-elution of C3 with carbonate in the IC  
416 analysis. Glutarate (C5) was also excluded from the analysis due to very low concentrations. For  
417 the examination of the organic species, MO8 was again separated from the other MOUDI sets  
418 due to it having the second highest concentration of organic species ( $0.66 \mu\text{g m}^{-3}$ ) and an organic  
419 species contribution profile very similar to that of MO7. The remaining MOUDI sets included in

420 the average category (MO1 – MO6, MO9 – MO10) all have total organic species concentrations  
421 that were less than the four highest aerosol sets (MO7, MO8, MO12, MO14) and greater than the  
422 lowest aerosol set (MO11). The lowest aerosol event (MO11) has the lowest overall  
423 concentration of organic aerosol ( $0.09 \mu\text{g m}^{-3}$ ), while the 2<sup>nd</sup> highest aerosol event (MO7) has the  
424 highest concentration of organic aerosol ( $0.70 \mu\text{g m}^{-3}$ ).

425 Many studies worldwide have examined the relative contributions of organic species to  
426 atmospheric aerosol, with oxalate typically having the highest contribution among dicarboxylic  
427 acids (Kawamura and Kaplan, 1987; Kawamura and Ikushima, 1993; Kawamura and Sakaguchi,  
428 1999; Sorooshian et al., 2007a; Hsieh et al., 2007, 2008; Aggarwal and Kawamura, 2008;  
429 Deshmukh et al., 2012, 2018; Li et al., 2015; Hoque et al., 2017; Kunwar et al., 2019). Oxalate  
430 was the dominant water-soluble organic species for all 12 MOUDI sets, with oxalate having the  
431 highest contribution to the organic aerosol in MO12 (88.7% of total organic aerosol). Oxalate is  
432 often considered a byproduct of photochemical aging of longer-chain dicarboxylic acids (e.g.  
433 Kawamura and Ikushima, 1993; Kawamura and Sakaguchi, 1999), and therefore an increase in  
434 oxalate is often considered a signature of aged aerosol in the absence of primary oxalate  
435 emissions from sources such as biomass burning. Another major pathway of oxalate formation is  
436 aqueous processing (Crahan et al., 2004; Ervens et al., 2004, 2018; Sorooshian et al., 2006,  
437 2007b; Wonaschuetz et al., 2012), which is likely prevalent during the SWM when there is  
438 frequent cloud cover. Previous studies have also demonstrated the ability for transport of and  
439 photochemical aging of water-soluble organic acids over long distances in a marine environment  
440 (e.g. Kawamura and Sakaguchi, 1999) and the importance of emissions from continental Asia in  
441 the organic aerosol budget in the western north Pacific (Aggarwal and Kawamura, 2008; Hoque  
442 et al., 2017). The back-trajectories of the air masses terminating at MO during MO12 and MO14  
443 indicate origins of emissions from continental East Asia (Figure 2). It is plausible that the high  
444 contribution of oxalate to the organic aerosol in MO12 and MO14 (which had the fourth highest  
445 percent contribution of oxalate) is due to the degradation of both primarily-emitted and  
446 secondarily-produced longer-chain dicarboxylic acids during the transport process through  
447 mechanisms described above, such as photochemical degradation and aqueous processing, with  
448 the former mechanism being plausible in the regions of low cloud cover to the north and  
449 northwest of the Manila (Figure 1) and the latter mechanism potentially being of great  
450 importance due to the typhoon influences during transport. While the aerosol measured in MO7  
451 and MO8 also show long-range transport influences (Figure 2a and Figure S1), the overall signal  
452 of organic aerosol is much stronger in these two sets, such that the absolute concentration of  
453 oxalate (MO7:  $0.47 \mu\text{g m}^{-3}$  and MO8:  $0.42 \mu\text{g m}^{-3}$ ) is still greater than in MO12 ( $0.19 \mu\text{g m}^{-3}$ )  
454 and MO14 ( $0.37 \mu\text{g m}^{-3}$ ). However, biomass burning is a well-documented source of both  
455 oxalate and longer-chain dicarboxylic acids (e.g. Falkovich et al., 2005; Nirmalkar et al., 2015;  
456 Cheng et al., 2017; Deshmukh et al., 2018; Thepnuan et al., 2019).

457 Succinate has been linked to biomass burning emissions (Wang and Shooter, 2004;  
458 Falkovich et al., 2005; Zhao et al., 2014; Balla et al., 2018), vehicular emissions (Kawamura and  
459 Kaplan, 1987; Kawamura et al., 1996; Yao et al., 2004), and secondary production via  
460 photochemical reactions of precursor organic compounds (Kawamura and Ikushima, 1993;  
461 Kawamura et al., 1996; Kawamura and Sakaguchi, 1999). The two MO MOUDI sets thought to  
462 have the most influence from biomass burning emissions (MO7 and MO8) had the highest  
463 organic aerosol mass concentrations and the highest mass percent contributions of succinate to  
464 the organic aerosol (MO7: 14.3% and MO8: 17.5%). In contrast, the next highest contribution of  
465 succinate to the organic aerosol was 4.2% measured in MO5. These results agree with previous

466 studies in Northeast China that showed an increase in total organic aerosol mass concentration  
467 and a strong increase (decrease) in the relative contribution of succinate (oxalate) during biomass  
468 burning periods as opposed to non-biomass burning periods (Cao et al., 2017). Results from  
469 California, USA also showed higher percent contributions of succinate to the water-soluble  
470 organic aerosol during periods influenced by biomass burning (Maudlin et al., 2015).

471 MO11 had the second highest relative contribution of maleate (28.5% of water-soluble  
472 organic aerosol) out of all 12 sample sets and had a much higher percent contribution as  
473 compared to the four highest aerosol events (<2.5% for each of the following: MO7, MO8,  
474 MO12, and MO14). Maleate is linked to the oxidation of aromatic hydrocarbons, usually from  
475 anthropogenic sources such as vehicular emissions (Kawamura and Kaplan, 1987; Kunwar et al.,  
476 2019). One explanation for this result could be the higher rainfall accumulation in and around the  
477 study region during MO11 as compared to the three highest aerosol sets (Figure 2). Wet  
478 scavenging could have removed aerosol from transported air masses during their journey towards  
479 MO, thereby increasing the relative contribution of local sources to the measured aerosol in  
480 MO11. Because of the reduced aging time associated with emissions from local sources, the  
481 relative increase in the contribution of longer-chain dicarboxylic acids and the decrease in the  
482 relative contribution of oxalate is plausible. Hsieh et al. (2008) showed in samples from Taiwan  
483 that the relative contribution of oxalate to the organic acids was also higher during periods of  
484 high aerosol loading as opposed to periods of moderate aerosol loading when the overall PM  
485 concentration was lower. MO11, which showed air mass back-trajectories originating to the east  
486 of the Philippines from the open Pacific (Figure 2b), had the lowest overall water-soluble PM  
487 concentration, the lowest overall concentration of water-soluble organic acids, and the second  
488 lowest percent contribution of oxalate to the organic acid mass (57.1%) of all the sets.

489 Phthalate is an aromatic dicarboxylic acid often linked to anthropogenic sources through  
490 photochemical transformation of emissions from vehicles (Kawamura and Kaplan, 1987;  
491 Kawamura and Ikushima, 1993) and waste burning (Kumar et al., 2015), although aqueous  
492 processing has also been proposed as a formation mechanism (Kunwar et al., 2019).  
493 Accordingly, phthalate has been shown to have seasonal and diurnal variations in concentration,  
494 with enhanced production usually linked to times of stronger solar radiation (i.e. summertime  
495 and daytime: Satsumabayashi et al., 1990; Ray and McDow, 2005; Ho et al., 2006; Kunwar et  
496 al., 2019). However, increased emissions of precursor species during different times of the year  
497 may affect these trends (Hyder et al., 2012). Sets MO7, MO8, MO11, and MO14 had the highest  
498 contribution to the water-soluble organics from phthalate (range: 9.5 – 10.2%). In contrast, the  
499 remaining sets had a much lower contribution (range: 1.7 – 4.9%). However, the absolute  
500 concentration of phthalate was highest in sets MO7, MO8, and MO14 (range: 45.3 – 67.0 ng m<sup>-3</sup>)  
501 <sup>3</sup>), and much lower for the remaining sets (range: 2.0 – 8.9 ng m<sup>-3</sup>). Increased phthalate  
502 concentrations during biomass burning episodes have been previously measured in SE Asia (Cao  
503 et al., 2017). Furthermore, cloud coverage was fairly low during MO14 as compared to the other  
504 sets of interest (Figure 1), increasing the possibility of photochemical production of phthalate.  
505 For the remaining sample sets, the range of phthalate concentrations is substantially lower and  
506 fairly consistent, indicating that the measured phthalate in these samples most likely represents  
507 the local background conditions.

508 While not a carboxylic acid, MSA is nonetheless an important organic aerosol species,  
509 especially in marine environments. The assumed precursor of MSA in this study is from the  
510 oxidation of marine-emitted dimethylsulfide (DMS). Interestingly, all sample sets showed  
511 approximately the same mass percent contribution of MSA to the organic aerosol, ranging from a

512 minimum of 3.1% (MO6) to a maximum of 7.0% (MO5). However, the absolute concentration  
513 of MSA was highest in the two sets with biomass burning influence (MO7: 23.3 ng m<sup>-3</sup> and  
514 MO8: 21.4 ng m<sup>-3</sup>), with concentrations 8.4 and 7.7 times higher, respectively, than the lowest  
515 MSA concentration measured (MO11: 2.8 ng m<sup>-3</sup>). A previous study showed that MSA  
516 concentrations in air masses with mixed influence from marine and biomass burning emissions  
517 are higher than the concentrations measured from either source alone (Sorooshian et al., 2015).  
518 The results from the present study (i.e. more MSA measured in sets with biomass burning  
519 influence) in SE Asia again highlight the complexity of interactions between air masses with  
520 different sources and the accompanying changes in aerosol physiochemical properties.

521

#### 522 **4. Conclusions**

523 This study sought to characterize influences of local and long-range transported aerosol  
524 to the Philippines during the Southwest Monsoon (SWM) season as well as the various synoptic  
525 and local scale conditions that facilitate and suppress long-range transport of aerosol. As a highly  
526 populated mega-city, Metro Manila is the source of a large amount of urban, anthropogenic  
527 pollution. However, synoptic-scale weather, including the typical SWM flow and typhoons, can  
528 impact the transport of aerosol to and from Metro Manila. While previous work in a rural area in  
529 the northwest edge of the Philippines has identified seasonal aerosol transport patterns to the  
530 Philippines using PM<sub>2.5</sub> data (Bagtasa et al., 2018), the present study highlights case studies of in  
531 situ size-resolved aerosol measurements from Metro Manila to examine the potential for aerosol  
532 transport to impact this urban area as well.

533 For two of the sample sets with enhanced total water-soluble aerosol mass concentration,  
534 biomass burning aerosol transport from the Maritime Continent (MC) towards the Philippines  
535 was identified using air mass back-trajectories and the Navy Aerosol Analysis and Prediction  
536 System (NAAPS) model. This transport followed a southwesterly flow pattern that is typical of  
537 this time of year (Figure S1) and lends its name to the SWM season. Deep aerosol layers,  
538 extending from the surface to 3 km, were identified by CALIOP to the southwest of the  
539 Philippines. The influence on aerosol in Metro Manila was shown through enhancements in  
540 biomass burning tracer species (e.g. K, Rb) and increased concentration of organic aerosol. The  
541 challenges in satellite-based retrievals of biomass burning in the region (Reid et al., 2012, 2013)  
542 and the underestimation of fire activity in the region by these satellite retrievals (Reid et al.,  
543 2013) lead to unanswered questions about the amount and fate of biomass burning emissions in  
544 the MC and SE Asia. The ability to measure biomass burning signatures in a highly polluted,  
545 urban mega-city such as Metro Manila and the evidence of long-range transport gathered through  
546 multiple methods and data sources (i.e. in situ measurements, models, and remote-sensing)  
547 speaks to the strong signature of biomass burning emissions in the region and the long-range  
548 transport pathways available for these emissions.

549 In contrast, transport of anthropogenic emissions from continental East Asia was  
550 identified on two occasions with high water-soluble aerosol mass concentrations, with one  
551 measured instance of long-range transport having been facilitated by the influence of a typhoon.  
552 In these cases, it is difficult to separate urban emissions between local and distant sources.  
553 However, the elevation of select tracer species (Ba, V, Pb, Mo, Sn) and the water-soluble organic  
554 aerosol characteristics for these two cases (i.e. high relative contribution of oxalate to the organic  
555 aerosol) indicated that long-range transported urban emissions could impact Metro Manila.

556 Finally, one low aerosol loading case was impacted by air masses travelling over the  
557 open ocean to the east of the Philippines. This case showed an enhanced fraction of

558 supermicrometer aerosol and a very low concentration of water-soluble organic acids. Higher  
559 rain accumulation during this sample set, as opposed to the sample sets with the highest water-  
560 soluble aerosol concentrations, could have led to greater wet scavenging of aerosol. This case  
561 also had the lowest overall mass concentration of water-soluble organic species, a low percent  
562 contribution of oxalate to the water-soluble organics, and a high percent contribution of maleate.  
563 This result points to the relative importance of locally-emitted species that have not yet  
564 undergone photochemical and aqueous processing mechanisms that lead to the degradation of  
565 longer-chain dicarboxylic acid species into oxalate.

566 These results have important implications for better understanding the aerosol budget and  
567 influences in and around the Philippines and SE Asia. Transport of aerosol both into and out of  
568 Metro Manila can impact human health, cloud condensation nuclei (CCN) budgets, and radiative  
569 forcing in the region. Furthermore, the identification of various tracer species (e.g. K and Rb for  
570 biomass burning) and the impacts of different long-range transport mechanisms, ~~and associated~~  
571 have worldwide applications. In addition, the mixing of different air mass types, ~~on the water-~~  
572 soluble ~~resulting in changes in~~ aerosol characteristics (e.g. enhanced oxalate in emissions from  
573 continental regions, enhanced MSA during periods of biomass burning influence) ~~have~~  
574 worldwide applications. ~~is a subject that requires more attention on a global basis. While this~~  
575 work has shown the influence of mixing biomass burning emissions and urban emissions, from  
576 both local and more distant urban centers, additional analysis at the study site has demonstrated  
577 the influences seen from the mixing of sea salt aerosol with other airmasses (AzadiAghdam et  
578 al., 2019). As remote-sensing measurements in this region are notoriously difficult (e.g. Reid et  
579 al., 2009, 2013), in situ and model results lend vital data to address the questions surrounding  
580 characteristics of aerosol that are transported into and out of this highly-populated region.  
581 Measurements from in situ airborne campaigns, such as CAMP<sup>2</sup>Ex, can further address the  
582 changes in aerosol physicochemical characteristics that occur during long-range transport and  
583 aging in the atmosphere in the region.

584  
585 *Data availability:* All data used in this work are available upon request.

586  
587 *Author Contribution:* MTC, MOC, JBS, RAB, ABM, CS, and AS designed the experiments and  
588 all co-authors carried out some aspect of the data collection. MTC, RAB, CS, and AS conducted  
589 data analysis and interpretation. RAB and AS prepared the manuscript with contributions from  
590 all co-authors.

591  
592 *Competing interests:* The authors declare that they have no conflict of interest.

593  
594 *Acknowledgements:* This research was funded by NASA grant 80NSSC18K0148. R. A. Braun  
595 acknowledges support from the ARCS Foundation. M. T. Cruz acknowledges support from the  
596 Philippine Department of Science and Technology's ASTHRD Program. A. B. MacDonald  
597 acknowledges support from the Mexican National Council for Science and Technology  
598 (CONACYT). We acknowledge Agilent Technologies for their support and Shane Snyder's  
599 laboratories for ICP-QQQ data.

600  
601 **References**

602

603 Aggarwal, S. G., and Kawamura, K.: Molecular distributions and stable carbon isotopic  
604 compositions of dicarboxylic acids and related compounds in aerosols from Sapporo, Japan:  
605 Implications for photochemical aging during long-range atmospheric transport, *J. Geophys. Res.-*  
606 *Atmos.*, 113, 10.1029/2007jd009365, 2008.

607  
608 Agrawal, H., Malloy, Q. G. J., Welch, W. A., Wayne Miller, J., and Cocker, D. R.: In-use  
609 gaseous and particulate matter emissions from a modern ocean going container vessel, *Atmos.*  
610 *Environ.*, 42, 5504-5510, <https://doi.org/10.1016/j.atmosenv.2008.02.053>, 2008.

611  
612 Akagi, S. K., Craven, J. S., Taylor, J. W., McMeeking, G. R., Yokelson, R. J., Burling, I. R.,  
613 Urbanski, S. P., Wold, C. E., Seinfeld, J. H., Coe, H., Alvarado, M. J., and Weise, D. R.:  
614 Evolution of trace gases and particles emitted by a chaparral fire in California, *Atmos. Chem.*  
615 *Phys.*, 12, 1397-1421, 10.5194/acp-12-1397-2012, 2012.

616  
617 Alas, H. D., Müller, T., Birmili, W., Kecorius, S., Cambaliza, M. O., Simpas, J. B. B., Cayetano,  
618 M., Weinhold, K., Vallar, E., Galvez, M. C., and Wiedensohler, A.: Spatial Characterization of  
619 Black Carbon Mass Concentration in the Atmosphere of a Southeast Asian Megacity: An Air  
620 Quality Case Study for Metro Manila, Philippines, *Aerosol Air Qual. Res.*, 18, 2301-2317,  
621 10.4209/aaqr.2017.08.0281, 2018.

622  
623 Allen, A. G., Nemitz, E., Shi, J. P., Harrison, R. M., and Greenwood, J. C.: Size distributions of  
624 trace metals in atmospheric aerosols in the United Kingdom, *Atmos. Environ.*, 35, 4581-4591,  
625 [https://doi.org/10.1016/S1352-2310\(01\)00190-X](https://doi.org/10.1016/S1352-2310(01)00190-X), 2001.

626  
627 Amato, F., Pandolfi, M., Viana, M., Querol, X., Alastuey, A., and Moreno, T.: Spatial and  
628 chemical patterns of PM<sub>10</sub> in road dust deposited in urban environment, *Atmos. Environ.*, 43,  
629 1650-1659, <https://doi.org/10.1016/j.atmosenv.2008.12.009>, 2009.

630  
631 Andreae, M. O.: Soot Carbon and Excess Fine Potassium: Long-Range Transport of  
632 Combustion-Derived Aerosols, *Science*, 220, 1148, 10.1126/science.220.4602.1148, 1983.

633  
634 Arimoto, R., Duce, R. A., Ray, B. J., Ellis Jr, W. G., Cullen, J. D., and Merrill, J. T.: Trace  
635 elements in the atmosphere over the North Atlantic, *J. Geophys. Res.-Atmos.*, 100, 1199-1213,  
636 10.1029/94jd02618, 1995.

637  
638 Artaxo, P., Gerab, F., Yamasoe, M. A., and Martins, J. V.: Fine mode aerosol composition at  
639 three long-term atmospheric monitoring sites in the Amazon Basin, *J. Geophys. Res.-Atmos.*, 99,  
640 22857-22868, 10.1029/94jd01023, 1994.

641  
642 Artaxo, P., Oyola, P., and Martinez, R.: Aerosol composition and source apportionment in  
643 Santiago de Chile, *Nucl. Instrum. Meth. B*, 150, 409-416, [https://doi.org/10.1016/S0168-](https://doi.org/10.1016/S0168-583X(98)01078-7)  
644 [583X\(98\)01078-7](https://doi.org/10.1016/S0168-583X(98)01078-7), 1999.

645  
646 Atwood, S. A., Reid, J. S., Kreidenweis, S. M., Cliff, S. S., Zhao, Y., Lin, N.-H., Tsay, S.-C.,  
647 Chu, Y.-C., and Westphal, D. L.: Size resolved measurements of springtime aerosol particles



648 over the northern South China Sea, *Atmos. Environ.*, 78, 134-143,  
649 <https://doi.org/10.1016/j.atmosenv.2012.11.024>, 2013.  
650  
651 Atwood, S. A., Reid, J. S., Kreidenweis, S. M., Blake, D. R., Jonsson, H. H., Lagrosas, N. D.,  
652 Xian, P., Reid, E. A., Sessions, W. R., and Simpas, J. B.: Size-resolved aerosol and cloud  
653 condensation nuclei (CCN) properties in the remote marine South China Sea – Part 1:  
654 Observations and source classification, *Atmos. Chem. Phys.*, 17, 1105-1123, 10.5194/acp-17-  
655 1105-2017, 2017.  
656  
657 [AzadiAghdam, M., Braun, R. A., Edwards, E.-L., Bañaga, P. A., Cruz, M. T., Betito, G.,](#)  
658 [Cambaliza, M. O., Dadashazar, H., Lorenzo, G. R., Ma, L., MacDonald, A. B., Nguyen, P.,](#)  
659 [Simpas, J. B., Stahl, C., and Sorooshian, A.: On the nature of sea salt aerosol at a coastal](#)  
660 [megacity: Insights from Manila, Philippines in Southeast Asia, \*Atmos. Environ.\*, 216, 116922,](#)  
661 [<https://doi.org/10.1016/j.atmosenv.2019.116922>, 2019.](#)  
662 [Bagtasa, G.: Effect of Synoptic Scale Weather Disturbance to Philippine Transboundary Oxone](#)  
663 [Pollution using WRF-CHEM. \*Int. J. Environ. Sci. Dev.\*, 2, 402-405,](#)  
664 [\[10.7763/IJESD.2011.V2.159\]\(https://doi.org/10.7763/IJESD.2011.V2.159\), 2011.](#)  
665  
666 Bagtasa, G., Cayetano, M. G., and Yuan, C. S.: Seasonal variation and chemical characterization  
667 of PM<sub>2.5</sub> in northwestern Philippines, *Atmos. Chem. Phys.*, 18, 4965-4980, 10.5194/acp-18-  
668 4965-2018, 2018.  
669  
670 Balla, D., Voutsas, D., and Samara, C.: Study of polar organic compounds in airborne particulate  
671 matter of a coastal urban city, *Environ. Sci. Pollut. R.*, 25, 12191-12205, 10.1007/s11356-017-  
672 9993-2, 2018.  
673  
674 Bautista, A. T., Pabroa, P. C. B., Santos, F. L., Racho, J. M. D., and Quirit, L. L.: Carbonaceous  
675 particulate matter characterization in an urban and a rural site in the Philippines, *Atmos. Pollut.*  
676 *Res.*, 5, 245-252, <https://doi.org/10.5094/APR.2014.030>, 2014.  
677  
678 Bovallius, A., Bucht, B., Roffey, R., and Anäs, P.: Long-range air transmission of bacteria, *Appl.*  
679 *Environ. Microb.*, 35, 1231, 1978.  
680  
681 Braun, R. A., Dadashazar, H., MacDonald, A. B., Aldhaif, A. M., Maudlin, L. C., Crosbie, E.,  
682 Aghdam, M. A., Hossein Mardi, A., and Sorooshian, A.: Impact of Wildfire Emissions on  
683 Chloride and Bromide Depletion in Marine Aerosol Particles, *Environ. Sci. Technol.*, 51, 9013-  
684 9021, 10.1021/acs.est.7b02039, 2017.  
685  
686 Brito, J., Freney, E., Dominutti, P., Borbon, A., Haslett, S. L., Batenburg, A. M., Colomb, A.,  
687 Dupuy, R., Denjean, C., Burnet, F., Bourriane, T., Deroubaix, A., Sellegri, K., Borrmann, S.,  
688 Coe, H., Flamant, C., Knippertz, P., and Schwarzenboeck, A.: Assessing the role of  
689 anthropogenic and biogenic sources on PM<sub>1</sub> over southern West Africa using aircraft  
690 measurements, *Atmos. Chem. Phys.*, 18, 757-772, 10.5194/acp-18-757-2018, 2018.  
691

692 Campbell, J. R., Reid, J. S., Westphal, D. L., Zhang, J., Tackett, J. L., Chew, B. N., Welton, E. J.,  
693 Shimizu, A., Sugimoto, N., Aoki, K., and Winker, D. M.: Characterizing the vertical profile of  
694 aerosol particle extinction and linear depolarization over Southeast Asia and the Maritime  
695 Continent: The 2007–2009 view from CALIOP, *Atmos. Res.*, 122, 520-543,  
696 <https://doi.org/10.1016/j.atmosres.2012.05.007>, 2013.  
697

698 Cao, F., Zhang, S.-C., Kawamura, K., Liu, X., Yang, C., Xu, Z., Fan, M., Zhang, W., Bao, M.,  
699 Chang, Y., Song, W., Liu, S., Lee, X., Li, J., Zhang, G., and Zhang, Y.-L.: Chemical  
700 characteristics of dicarboxylic acids and related organic compounds in PM<sub>2.5</sub> during biomass-  
701 burning and non-biomass-burning seasons at a rural site of Northeast China, *Environ. Pollut.*,  
702 231, 654-662, <https://doi.org/10.1016/j.envpol.2017.08.045>, 2017.  
703

704 Cayan, E. O., Chen, T.-C., Argete, J. C., Yen, M.-C., and Nilo, P. D.: The Effect of Tropical  
705 Cyclones on Southwest Monsoon Rainfall in the Philippines, *J. Meteorol. Soc. Jpn. Ser. II*, 89A,  
706 123-139, 10.2151/jmsj.2011-A08, 2011.  
707

708 Chang, L. T.-C., Tsai, J.-H., Lin, J.-M., Huang, Y.-S., and Chiang, H.-L.: Particulate matter and  
709 gaseous pollutants during a tropical storm and air pollution episode in Southern Taiwan, *Atmos.*  
710 *Res.*, 99, 67-79, <https://doi.org/10.1016/j.atmosres.2010.09.002>, 2011.  
711

712 Cheng, C., Li, M., Chan, C. K., Tong, H., Chen, C., Chen, D., Wu, D., Li, L., Wu, C., Cheng, P.,  
713 Gao, W., Huang, Z., Li, X., Zhang, Z., Fu, Z., Bi, Y., and Zhou, Z.: Mixing state of oxalic acid  
714 containing particles in the rural area of Pearl River Delta, China: implications for the formation  
715 mechanism of oxalic acid, *Atmos. Chem. Phys.*, 17, 9519-9533, 10.5194/acp-17-9519-2017,  
716 2017.  
717

718 Chow, J. C., Watson, J. G., Kuhns, H., Etyemezian, V., Lowenthal, D. H., Crow, D., Kohl, S. D.,  
719 Engelbrecht, J. P., and Green, M. C.: Source profiles for industrial, mobile, and area sources in  
720 the Big Bend Regional Aerosol Visibility and Observational study, *Chemosphere*, 54, 185-208,  
721 <https://doi.org/10.1016/j.chemosphere.2003.07.004>, 2004.  
722

723 Chuang, M.-T., Chang, S.-C., Lin, N.-H., Wang, J.-L., Sheu, G.-R., Chang, Y.-J., and Lee, C.-T.:  
724 Aerosol chemical properties and related pollutants measured in Dongsha Island in the northern  
725 South China Sea during 7-SEAS/Dongsha Experiment, *Atmos. Environ.*, 78, 82-92,  
726 <https://doi.org/10.1016/j.atmosenv.2012.05.014>, 2013.  
727

728 Crahan, K. K., Hegg, D., Covert, D. S., and Jonsson, H.: An exploration of aqueous oxalic acid  
729 production in the coastal marine atmosphere, *Atmos. Environ.*, 38, 3757-3764,  
730 <https://doi.org/10.1016/j.atmosenv.2004.04.009>, 2004.  
731

732 Cruz, F. T., Narisma, G. T., Villafuerte, M. Q., Cheng Chua, K. U., and Olaguera, L. M.: A  
733 climatological analysis of the southwest monsoon rainfall in the Philippines, *Atmos. Res.*, 122,  
734 609-616, <https://doi.org/10.1016/j.atmosres.2012.06.010>, 2013.  
735

736 Cruz, M. T., Bañaga, P. A., Betito, G., Braun, R. A., Stahl, C., Aghdam, M. A., Cambaliza, M.  
737 O., Dadashazar, H., Hilario, M. R., Lorenzo, G. R., Ma, L., MacDonald, A. B., Pabroa, P. C.,

738 Yee, J. R., Simpas, J. B., and Sorooshian, A.: Size-resolved Composition and Morphology of  
739 Particulate Matter During the Southwest Monsoon in Metro Manila, Philippines, *Atmos. Chem.*  
740 *Phys.*, 19, 10675-10696, <https://doi.org/10.5194/acp-19-10675-2019>, 2019.  
741  
742 Dave, P., Bhushan, M., and Venkataraman, C.: Aerosols cause intraseasonal short-term  
743 suppression of Indian monsoon rainfall, *Sci. Rep.-UK*, 7, 17347, 10.1038/s41598-017-17599-1,  
744 2017.  
745  
746 Deshmukh, D. K., Deb, M. K., Hopke, P. K., and Tsai, Y. I.: Seasonal Characteristics of Water-  
747 Soluble Dicarboxylates Associated with PM10 in the Urban Atmosphere of Durg City, India,  
748 *Aerosol Air Qual. Res.*, 12, 683-696, 10.4209/aaqr.2012.02.0040, 2012.  
749  
750 Deshmukh, D. K., Mozammel Haque, M., Kawamura, K., and Kim, Y.: Dicarboxylic acids,  
751 oxocarboxylic acids and  $\alpha$ -dicarbonyls in fine aerosols over central Alaska: Implications for  
752 sources and atmospheric processes, *Atmos. Res.*, 202, 128-139,  
753 <https://doi.org/10.1016/j.atmosres.2017.11.003>, 2018.  
754  
755 Duce, R. A., Liss, P. S., Merrill, J. T., Atlas, E. L., Buat-Menard, P., Hicks, B. B., Miller, J. M.,  
756 Prospero, J. M., Arimoto, R., Church, T. M., Ellis, W., Galloway, J. N., Hansen, L., Jickells, T.  
757 D., Knap, A. H., Reinhardt, K. H., Schneider, B., Soudine, A., Tokos, J. J., Tsunogai, S.,  
758 Wollast, R., and Zhou, M.: The atmospheric input of trace species to the world ocean, *Global*  
759 *Biogeochem. Cy.*, 5, 193-259, 10.1029/91gb01778, 1991.  
760  
761 Echalar, F., Gaudichet, A., Cachier, H., and Artaxo, P.: Aerosol emissions by tropical forest and  
762 savanna biomass burning: Characteristic trace elements and fluxes, *Geophys. Res. Lett.*, 22,  
763 3039-3042, 10.1029/95gl03170, 1995.  
764  
765 Ervens, B.: Modeling the Processing of Aerosol and Trace Gases in Clouds and Fogs, *Chem.*  
766 *Rev.*, 115, 4157-4198, 10.1021/cr5005887, 2015.  
767  
768 Ervens, B., Feingold, G., Frost, G. J., and Kreidenweis, S. M.: A modeling study of aqueous  
769 production of dicarboxylic acids: 1. Chemical pathways and speciated organic mass production,  
770 *J. Geophys. Res.-Atmos.*, 109, 10.1029/2003jd004387, 2004.  
771  
772 Ervens, B., Sorooshian, A., Aldhaif, A. M., Shingler, T., Crosbie, E., Ziemba, L., Campuzano-  
773 Jost, P., Jimenez, J. L., and Wisthaler, A.: Is there an aerosol signature of chemical cloud  
774 processing?, *Atmos. Chem. Phys.*, 18, 16099-16119, 10.5194/acp-18-16099-2018, 2018.  
775  
776 Falkovich, A. H., Graber, E. R., Schkolnik, G., Rudich, Y., Maenhaut, W., and Artaxo, P.: Low  
777 molecular weight organic acids in aerosol particles from Rondônia, Brazil, during the biomass-  
778 burning, transition and wet periods, *Atmos. Chem. Phys.*, 5, 781-797, 10.5194/acp-5-781-2005,  
779 2005.  
780  
781 Fang, G.-C., Lin, S.-J., Chang, S.-Y., and Chou, C.-C. K.: Effect of typhoon on atmospheric  
782 particulates in autumn in central Taiwan, *Atmos. Environ.*, 43, 6039-6048,  
783 <https://doi.org/10.1016/j.atmosenv.2009.08.033>, 2009.

784  
785 Farren, N. J., Dunmore, R. E., Mead, M. I., Mohd Nadzir, M. S., Samah, A. A., Phang, S. M.,  
786 Bandy, B. J., Sturges, W. T., and Hamilton, J. F.: Chemical characterisation of water-soluble  
787 ions in atmospheric particulate matter on the east coast of Peninsular Malaysia, *Atmos. Chem.*  
788 *Phys.*, 19, 1537-1553, 10.5194/acp-19-1537-2019, 2019.  
789  
790 Flannigan, M. D., Krawchuk, M. A., de Groot, W. J., Wotton, B. M., and Gowman, L. M.:  
791 Implications of changing climate for global wildland fire, *Int. J. Wildland Fire*, 18, 483-507,  
792 <https://doi.org/10.1071/WF08187>, 2009.  
793  
794 Flannigan, M., Cantin, A. S., de Groot, W. J., Wotton, M., Newbery, A., and Gowman, L. M.:  
795 Global wildland fire season severity in the 21st century, *Forest Ecol. Manag.*, 294, 54-61,  
796 <https://doi.org/10.1016/j.foreco.2012.10.022>, 2013.  
797  
798 Fujimori, T., Takigami, H., Agusa, T., Eguchi, A., Bekki, K., Yoshida, A., Terazono, A., and  
799 Ballesteros, F. C.: Impact of metals in surface matrices from formal and informal electronic-  
800 waste recycling around Metro Manila, the Philippines, and intra-Asian comparison, *J. Hazard.*  
801 *Mater.*, 221-222, 139-146, <https://doi.org/10.1016/j.jhazmat.2012.04.019>, 2012.  
802  
803 Fung, Y. S., and Wong, L. W. Y.: Apportionment of air pollution sources by receptor models in  
804 Hong Kong, *Atmos. Environ.*, 29, 2041-2048, [https://doi.org/10.1016/1352-2310\(94\)00239-H](https://doi.org/10.1016/1352-2310(94)00239-H),  
805 1995.  
806  
807 Gadde, B., Bonnet, S., Menke, C., and Garivait, S.: Air pollutant emissions from rice straw open  
808 field burning in India, Thailand and the Philippines, *Environ. Pollut.*, 157, 1554-1558,  
809 <https://doi.org/10.1016/j.envpol.2009.01.004>, 2009.  
810  
811 Ge, C., Wang, J., Reid, J. S., Posselt, D. J., Xian, P., and Hyer, E.: Mesoscale modeling of smoke  
812 transport from equatorial Southeast Asian Maritime Continent to the Philippines: First  
813 comparison of ensemble analysis with in situ observations, *J. Geophys. Res.-Atmos.*, 122, 5380-  
814 5398, doi:10.1002/2016JD026241, 2017.  
815  
816 Gelaro, R., McCarty, W., Suárez, M. J., Todling, R., Molod, A., Takacs, L., Randles, C. A.,  
817 Darmenov, A., Bosilovich, M. G., Reichle, R., Wargan, K., Coy, L., Cullather, R., Draper, C.,  
818 Akella, S., Buchard, V., Conaty, A., Silva, A. M. d., Gu, W., Kim, G.-K., Koster, R., Lucchesi,  
819 R., Merkova, D., Nielsen, J. E., Partyka, G., Pawson, S., Putman, W., Rienecker, M., Schubert,  
820 S. D., Sienkiewicz, M., and Zhao, B.: The Modern-Era Retrospective Analysis for Research and  
821 Applications, Version 2 (MERRA-2), *J. Climate*, 30, 5419-5454, 10.1175/jcli-d-16-0758.1,  
822 2017.  
823  
824 Global Modeling and Assimilation Office (GMAO): MERRA-2 inst3\_3d\_asm\_Nv: 3d,3-  
825 Hourly,Instantaneous,Model-Level,Assimilation,Assimilated Meteorological Fields V5.12.4,  
826 Goddard Earth Sciences Data and Information Services Center (GES DISC),  
827 10.5067/WWQSXQ8IVFW8, 2015a.  
828

829 Global Modeling and Assimilation Office (GMAO): MERRA-2 tavg1\_2d\_rad\_Nx: 2d,1-  
830 Hourly,Time-Averaged,Single-Level,Assimilation,Radiation Diagnostics V5.12.4, Goddard  
831 Earth Sciences Data and Information Services Center (GES DISC), 10.5067/Q9QMY5PBNV1T,  
832 2015b.

833  
834 Goldstein, A. H., Koven, C. D., Heald, C. L., and Fung, I. Y.: Biogenic carbon and  
835 anthropogenic pollutants combine to form a cooling haze over the southeastern United States, P.  
836 Natl. Acad. Sci. USA, 106, 8835-8840, 10.1073/pnas.0904128106, 2009.

837  
838 Graf, H. F., Yang, J., and Wagner, T. M.: Aerosol effects on clouds and precipitation during the  
839 1997 smoke episode in Indonesia, Atmos. Chem. Phys., 9, 743-756, 10.5194/acp-9-743-2009,  
840 2009.

841  
842 Ho, K. F., Lee, S. C., Cao, J. J., Kawamura, K., Watanabe, T., Cheng, Y., and Chow, J. C.:  
843 Dicarboxylic acids, ketocarboxylic acids and dicarbonyls in the urban roadside area of Hong  
844 Kong, Atmos. Environ., 40, 3030-3040, <https://doi.org/10.1016/j.atmosenv.2005.11.069>, 2006.

845  
846 Hogan, T. F., Liu, M., Ridout, J. A., Peng, M. S., Whitcomb, T. R., Ruston, B. C., Reynolds, C.  
847 A., Eckermann, S. D., Moskaitis, J. R., Baker, N. L., McCormack, J. P., Viner, K. C., McLay, J.  
848 G., Flatau, M. K., Xu, L., Chen, C., and Chang, S. W.: The Navy Global Environmental Model,  
849 Oceanography, 27, 116-125, <https://doi.org/10.5670/oceanog.2014.73>, 2014.

850  
851 Hong, Y., Hsu, K.-L., Sorooshian, S., and Gao, X.: Precipitation Estimation from Remotely  
852 Sensed Imagery Using an Artificial Neural Network Cloud Classification System, J. Appl.  
853 Meteorol., 43, 1834-1853, 10.1175/jam2173.1, 2004.

854  
855 Hoque, M. M. M., Kawamura, K., and Uematsu, M.: Spatio-temporal distributions of  
856 dicarboxylic acids,  $\omega$ -oxocarboxylic acids, pyruvic acid,  $\alpha$ -dicarbonyls and fatty acids in the  
857 marine aerosols from the North and South Pacific, Atmos. Res., 185, 158-168,  
858 <https://doi.org/10.1016/j.atmosres.2016.10.022>, 2017.

859  
860 Hsieh, L.-Y., Kuo, S.-C., Chen, C.-L., and Tsai, Y. I.: Origin of low-molecular-weight  
861 dicarboxylic acids and their concentration and size distribution variation in suburban aerosol,  
862 Atmos. Environ., 41, 6648-6661, <https://doi.org/10.1016/j.atmosenv.2007.04.014>, 2007.

863  
864 Hsieh, L.-Y., Chen, C.-L., Wan, M.-W., Tsai, C.-H., and Tsai, Y. I.: Speciation and temporal  
865 characterization of dicarboxylic acids in PM<sub>2.5</sub> during a PM episode and a period of non-  
866 episodic pollution, Atmos. Environ., 42, 6836-6850,  
867 <https://doi.org/10.1016/j.atmosenv.2008.05.021>, 2008.

868  
869 Hyder, M., Genberg, J., Sandahl, M., Swietlicki, E., and Jönsson, J. Å.: Yearly trend of  
870 dicarboxylic acids in organic aerosols from south of Sweden and source attribution, Atmos.  
871 Environ., 57, 197-204, <https://doi.org/10.1016/j.atmosenv.2012.04.027>, 2012.

872  
873 Jeong, C.-H., Wang, J. M., Hilker, N., Debosz, J., Sofowote, U., Su, Y., Noble, M., Healy, R. M.,  
874 Munoz, T., Dabek-Zlotorzynska, E., Celio, V., White, L., Audette, C., Herod, D., and Evans, G.

875 J.: Temporal and spatial variability of traffic-related PM<sub>2.5</sub> sources: Comparison of exhaust and  
876 non-exhaust emissions, *Atmos. Environ.*, 198, 55-69,  
877 <https://doi.org/10.1016/j.atmosenv.2018.10.038>, 2019.  
878

879 Juneng, L., Latif, M. T., and Tangang, F.: Factors influencing the variations of PM<sub>10</sub> aerosol  
880 dust in Klang Valley, Malaysia during the summer, *Atmos. Environ.*, 45, 4370-4378,  
881 <https://doi.org/10.1016/j.atmosenv.2011.05.045>, 2011.  
882

883 Kawamura, K., and Ikushima, K.: Seasonal changes in the distribution of dicarboxylic acids in  
884 the urban atmosphere, *Environ. Sci. Technol.*, 27, 2227-2235, 10.1021/es00047a033, 1993.  
885

886 Kawamura, K., and Kaplan, I. R.: Motor exhaust emissions as a primary source for dicarboxylic  
887 acids in Los Angeles ambient air, *Environ. Sci. Technol.*, 21, 105-110, 10.1021/es00155a014,  
888 1987.  
889

890 Kawamura, K., and Sakaguchi, F.: Molecular distributions of water soluble dicarboxylic acids in  
891 marine aerosols over the Pacific Ocean including tropics, *J. Geophys. Res.-Atmos.*, 104, 3501-  
892 3509, 10.1029/1998jd100041, 1999.  
893

894 Kawamura, K., Kasukabe, H., and Barrie, L. A.: Source and reaction pathways of dicarboxylic  
895 acids, ketoacids and dicarbonyls in arctic aerosols: One year of observations, *Atmos. Environ.*,  
896 30, 1709-1722, [https://doi.org/10.1016/1352-2310\(95\)00395-9](https://doi.org/10.1016/1352-2310(95)00395-9), 1996.  
897

898 Kecorius, S., Madueño, L., Vallar, E., Alas, H., Betito, G., Birmili, W., Cambaliza, M. O.,  
899 Catipay, G., Gonzaga-Cayetano, M., Galvez, M. C., Lorenzo, G., Müller, T., Simpas, J. B.,  
900 Tamayo, E. G., and Wiedensohler, A.: Aerosol particle mixing state, refractory particle number  
901 size distributions and emission factors in a polluted urban environment: Case study of Metro  
902 Manila, Philippines, *Atmos. Environ.*, 170, 169-183,  
903 <https://doi.org/10.1016/j.atmosenv.2017.09.037>, 2017.  
904

905 Kim, E., and Hopke, P. K.: Source characterization of ambient fine particles at multiple sites in  
906 the Seattle area, *Atmos. Environ.*, 42, 6047-6056,  
907 <https://doi.org/10.1016/j.atmosenv.2008.03.032>, 2008.  
908

909 Kim, J. Y., Ghim, Y. S., Song, C. H., Yoon, S.-C., and Han, J. S.: Seasonal characteristics of air  
910 masses arriving at Gosan, Korea, using fine particle measurements between November 2001 and  
911 August 2003, *J. Geophys. Res.-Atmos.*, 112, 10.1029/2005jd006946, 2007.  
912

913 Kim Oanh, N. T., Upadhyay, N., Zhuang, Y. H., Hao, Z. P., Murthy, D. V. S., Lestari, P.,  
914 Villarin, J. T., Chengchua, K., Co, H. X., Dung, N. T., and Lindgren, E. S.: Particulate air  
915 pollution in six Asian cities: Spatial and temporal distributions, and associated sources, *Atmos.*  
916 *Environ.*, 40, 3367-3380, <https://doi.org/10.1016/j.atmosenv.2006.01.050>, 2006.  
917

918 Kristiansen, N. I., Stohl, A., Olivie, D. J. L., Croft, B., Søvde, O. A., Klein, H., Christoudias, T.,  
919 Kunkel, D., Leadbetter, S. J., Lee, Y. H., Zhang, K., Tsigaridis, K., Bergman, T., Evangelidou, N.,  
920 Wang, H., Ma, P. L., Easter, R. C., Rasch, P. J., Liu, X., Pitari, G., Di Genova, G., Zhao, S. Y.,

921 Balkanski, Y., Bauer, S. E., Faluvegi, G. S., Kokkola, H., Martin, R. V., Pierce, J. R., Schulz, M.,  
922 Shindell, D., Tost, H., and Zhang, H.: Evaluation of observed and modelled aerosol lifetimes  
923 using radioactive tracers of opportunity and an ensemble of 19 global models, *Atmos. Chem.*  
924 *Phys.*, 16, 3525-3561, 10.5194/acp-16-3525-2016, 2016.

925  
926 Kumar, S., Aggarwal, S. G., Gupta, P. K., and Kawamura, K.: Investigation of the tracers for  
927 plastic-enriched waste burning aerosols, *Atmos. Environ.*, 108, 49-58,  
928 <https://doi.org/10.1016/j.atmosenv.2015.02.066>, 2015.

929  
930 Kunwar, B., Kawamura, K., Fujiwara, S., Fu, P., Miyazaki, Y., and Pokhrel, A.: Dicarboxylic  
931 acids, oxocarboxylic acids and  $\alpha$ -dicarbonyls in atmospheric aerosols from Mt. Fuji, Japan:  
932 Implication for primary emission versus secondary formation, *Atmos. Res.*, 221, 58-71,  
933 <https://doi.org/10.1016/j.atmosres.2019.01.021>, 2019.

934  
935 Latif, M. T., Othman, M., Idris, N., Juneng, L., Abdullah, A. M., Hamzah, W. P., Khan, M. F.,  
936 Nik Sulaiman, N. M., Jewaratnam, J., Aghamohammadi, N., Sahani, M., Xiang, C. J., Ahamad,  
937 F., Amil, N., Darus, M., Varkkey, H., Tangang, F., and Jaafar, A. B.: Impact of regional haze  
938 towards air quality in Malaysia: A review, *Atmos. Environ.*, 177, 28-44,  
939 <https://doi.org/10.1016/j.atmosenv.2018.01.002>, 2018.

940  
941 Li, X.-d., Yang, Z., Fu, P., Yu, J., Lang, Y.-c., Liu, D., Ono, K., and Kawamura, K.: High  
942 abundances of dicarboxylic acids, oxocarboxylic acids, and  $\alpha$ -dicarbonyls in fine aerosols  
943 (PM<sub>2.5</sub>) in Chengdu, China during wintertime haze pollution, *Environ. Sci. Pollut. R.*, 22,  
944 12902-12918, 10.1007/s11356-015-4548-x, 2015.

945  
946 Lin, C.-C., Chen, S.-J., Huang, K.-L., Hwang, W.-I., Chang-Chien, G.-P., and Lin, W.-Y.:  
947 Characteristics of Metals in Nano/Ultrafine/Fine/Coarse Particles Collected Beside a Heavily  
948 Trafficked Road, *Environ. Sci. Technol.*, 39, 8113-8122, 10.1021/es048182a, 2005.

949  
950 Lin, C. Y., Hsu, H. m., Lee, Y. H., Kuo, C. H., Sheng, Y. F., and Chu, D. A.: A new transport  
951 mechanism of biomass burning from Indochina as identified by modeling studies, *Atmos. Chem.*  
952 *Phys.*, 9, 7901-7911, 10.5194/acp-9-7901-2009, 2009.

953  
954 Lin, I. I., Chen, J.-P., Wong, G. T. F., Huang, C.-W., and Lien, C.-C.: Aerosol input to the South  
955 China Sea: Results from the MODerate Resolution Imaging Spectro-radiometer, the Quick  
956 Scatterometer, and the Measurements of Pollution in the Troposphere Sensor, *Deep-Sea Res. Pt.*  
957 *II*, 54, 1589-1601, <https://doi.org/10.1016/j.dsr2.2007.05.013>, 2007.

958  
959 Lindqvist, O., Johansson, K., Bringmark, L., Timm, B., Aastrup, M., Andersson, A., Hovsenius,  
960 G., Håkanson, L., Iverfeldt, Å., and Meili, M.: Mercury in the Swedish environment — Recent  
961 research on causes, consequences and corrective methods, *Water Air Soil Poll.*, 55, xi-261,  
962 10.1007/bf00542429, 1991.

963  
964 Liu, W., Han, Y., Yin, Y., Duan, J., Gong, J., Liu, Z., and Xu, W.: An aerosol air pollution  
965 episode affected by binary typhoons in east and central China, *Atmos. Pollut. Res.*, 9, 634-642,  
966 <https://doi.org/10.1016/j.apr.2018.01.005>, 2018.

967  
968 Liu, Y., Cai, W., Sun, C., Song, H., Cobb, K. M., Li, J., Leavitt, S. W., Wu, L., Cai, Q., Liu, R.,  
969 Ng, B., Cherubini, P., Büentgen, U., Song, Y., Wang, G., Lei, Y., Yan, L., Li, Q., Ma, Y., Fang,  
970 C., Sun, J., Li, X., Chen, D., and Linderholm, H. W.: Anthropogenic aerosols cause recent  
971 pronounced weakening of Asian Summer Monsoon relative to last four centuries, *Geophys. Res.*  
972 *Lett.*, 46, 10.1029/2019gl082497, 2019.

973  
974 Lu, C.-C., Yuan, C.-S., and Li, T.-C.: How Aeolian Dust Deteriorate Ambient Particulate Air  
975 Quality along an Expansive River Valley in Southern Taiwan? A Case Study of Typhoon  
976 Doksuri, *Aerosol Air Qual. Res.*, 17, 2181-2196, 10.4209/aaqr.2017.08.0257, 2017.

977  
978 Lynch, P., Reid, J. S., Westphal, D. L., Zhang, J., Hogan, T. F., Hyer, E. J., Curtis, C. A., Hegg,  
979 D. A., Shi, Y., Campbell, J. R., Rubin, J. I., Sessions, W. R., Turk, F. J., and Walker, A. L.: An  
980 11-year global gridded aerosol optical thickness reanalysis (v1.0) for atmospheric and climate  
981 sciences, *Geosci. Model Dev.*, 9, 1489-1522, 10.5194/gmd-9-1489-2016, 2016.

982  
983 Lyons, W. A., Dooley, J. C., and Whitby, K. T.: Satellite detection of long-range pollution  
984 transport and sulfate aerosol hazes, *Atmos. Environ. (1967)*, 12, 621-631,  
985 [https://doi.org/10.1016/0004-6981\(78\)90242-1](https://doi.org/10.1016/0004-6981(78)90242-1), 1978.

986  
987 Ma, L., Dadashazar, H., Braun, R. A., MacDonald, A. B., Aghdam, M. A., Maudlin, L. C., and  
988 Sorooshian, A.: Size-resolved Characteristics of Water-Soluble Particulate Elements in a Coastal  
989 Area: Source Identification, Influence of Wildfires, and Diurnal Variability, *Atmos. Environ.*,  
990 <https://doi.org/10.1016/j.atmosenv.2019.02.045>, 2019.

991  
992 Maenhaut, W., Salma, I., Cafmeyer, J., Annegarn, H. J., and Andreae, M. O.: Regional  
993 atmospheric aerosol composition and sources in the eastern Transvaal, South Africa, and impact  
994 of biomass burning, *J. Geophys. Res.-Atmos.*, 101, 23631-23650, 10.1029/95jd02930, 1996.

995  
996 Maki, T., Lee, K. C., Kawai, K., Onishi, K., Hong, C. S., Kurosaki, Y., Shinoda, M., Kai, K.,  
997 Iwasaka, Y., Archer, S. D. J., Lacap-Bugler, D. C., Hasegawa, H., and Pointing, S. B.: Aeolian  
998 dispersal of bacteria associated with desert dust and anthropogenic particles over continental and  
999 oceanic surfaces, *J. Geophys. Res.-Atmos.*, 124, 10.1029/2018jd029597, 2019.

1000  
1001 Mamoudou, I., Zhang, F., Chen, Q., Wang, P., and Chen, Y.: Characteristics of PM<sub>2.5</sub> from ship  
1002 emissions and their impacts on the ambient air: A case study in Yangshan Harbor, Shanghai, *Sci.*  
1003 *Total Environ.*, 640-641, 207-216, <https://doi.org/10.1016/j.scitotenv.2018.05.261>, 2018.

1004  
1005 Marple, V., Olson, B., Romay, F., Hudak, G., Geerts, S. M., and Lundgren, D.: Second  
1006 Generation Micro-Orifice Uniform Deposit Impactor, 120 MOUDI-II: Design, Evaluation, and  
1007 Application to Long-Term Ambient Sampling, *Aerosol Sci. Tech.*, 48, 427-433,  
1008 10.1080/02786826.2014.884274, 2014.

1009  
1010 Maudlin, L. C., Wang, Z., Jonsson, H. H., and Sorooshian, A.: Impact of wildfires on size-  
1011 resolved aerosol composition at a coastal California site, *Atmos. Environ.*, 119, 59-68,  
1012 <https://doi.org/10.1016/j.atmosenv.2015.08.039>, 2015.



1013  
1014 Moshier, B. W., and Duce, R. A.: A global atmospheric selenium budget, *J. Geophys. Res.-*  
1015 *Atmos.*, 92, 13289-13298, doi:10.1029/JD092iD11p13289, 1987.  
1016  
1017 Nguyen, P., Sellars, S., Thorstensen, A., Tao, Y., Ashouri, H., Braithwaite, D., Hsu, K., and  
1018 Sorooshian, S.: Satellites Track Precipitation of Super Typhoon Haiyan, *Eos Trans. AGU*, 95,  
1019 133-135, 10.1002/2014eo160002, 2014.  
1020  
1021 Nguyen, P., Shearer, E. J., Tran, H., Ombadi, M., Hayatbini, N., Palacios, T., Huynh, P.,  
1022 Braithwaite, D., Updegraff, G., Hsu, K., Kuligowski, B., Logan, W. S., and Sorooshian, S.: The  
1023 CHRS Data Portal, an easily accessible public repository for PERSIANN global satellite  
1024 precipitation data, *Scientific Data*, 6, 180296, 10.1038/sdata.2018.296, 2019.  
1025  
1026 Nirmalkar, J., Deshmukh, D. K., Deb, M. K., Tsai, Y. I., and Sopajaree, K.: Mass loading and  
1027 episodic variation of molecular markers in PM<sub>2.5</sub> aerosols over a rural area in eastern central  
1028 India, *Atmos. Environ.*, 117, 41-50, <https://doi.org/10.1016/j.atmosenv.2015.07.003>, 2015.  
1029  
1030 Nordø, J.: Long range transport of air pollutants in Europe and acid precipitation in Norway,  
1031 *Water Air Soil Poll.*, 6, 199-217, 10.1007/bf00182865, 1976.  
1032  
1033 Pakkanen, T. A., Loukkola, K., Korhonen, C. H., Aurela, M., Mäkelä, T., Hillamo, R. E., Aarnio,  
1034 P., Koskentalo, T., Kousa, A., and Maenhaut, W.: Sources and chemical composition of  
1035 atmospheric fine and coarse particles in the Helsinki area, *Atmos. Environ.*, 35, 5381-5391,  
1036 [https://doi.org/10.1016/S1352-2310\(01\)00307-7](https://doi.org/10.1016/S1352-2310(01)00307-7), 2001.  
1037  
1038 Pakkanen, T. A., Kerminen, V.-M., Loukkola, K., Hillamo, R. E., Aarnio, P., Koskentalo, T., and  
1039 Maenhaut, W.: Size distributions of mass and chemical components in street-level and rooftop  
1040 PM<sub>1</sub> particles in Helsinki, *Atmos. Environ.*, 37, 1673-1690, [https://doi.org/10.1016/S1352-](https://doi.org/10.1016/S1352-2310(03)00011-6)  
1041 [2310\(03\)00011-6](https://doi.org/10.1016/S1352-2310(03)00011-6), 2003.  
1042  
1043 Pandolfi, M., Gonzalez-Castanedo, Y., Alastuey, A., de la Rosa, J. D., Mantilla, E., de la Campa,  
1044 A. S., Querol, X., Pey, J., Amato, F., and Moreno, T.: Source apportionment of PM<sub>10</sub> and PM<sub>2.5</sub>  
1045 at multiple sites in the strait of Gibraltar by PMF: impact of shipping emissions, *Environ. Sci.*  
1046 *Pollut. R.*, 18, 260-269, 10.1007/s11356-010-0373-4, 2011.  
1047  
1048 Querol, X., Alastuey, A., Moreno, T., Viana, M. M., Castillo, S., Pey, J., Rodríguez, S.,  
1049 Artiñano, B., Salvador, P., Sánchez, M., Garcia Dos Santos, S., Herce Garraleta, M. D.,  
1050 Fernandez-Patier, R., Moreno-Grau, S., Negral, L., Minguillón, M. C., Monfort, E., Sanz, M. J.,  
1051 Palomo-Marín, R., Pinilla-Gil, E., Cuevas, E., de la Rosa, J., and Sánchez de la Campa, A.:  
1052 Spatial and temporal variations in airborne particulate matter (PM<sub>10</sub> and PM<sub>2.5</sub>) across Spain  
1053 1999–2005, *Atmos. Environ.*, 42, 3964-3979, <https://doi.org/10.1016/j.atmosenv.2006.10.071>,  
1054 2008.  
1055  
1056 Ray, J., and McDow, S. R.: Dicarboxylic acid concentration trends and sampling artifacts,  
1057 *Atmos. Environ.*, 39, 7906-7919, <https://doi.org/10.1016/j.atmosenv.2005.09.024>, 2005.  
1058

1059 Reid, J. S., Hyer, E. J., Prins, E. M., Westphal, D. L., Zhang, J., Wang, J., Christopher, S. A.,  
 1060 Curtis, C. A., Schmidt, C. C., Eleuterio, D. P., Richardson, K. A., and Hoffman, J. P.: Global  
 1061 Monitoring and Forecasting of Biomass-Burning Smoke: Description of and Lessons From the  
 1062 Fire Locating and Modeling of Burning Emissions (FLAMBE) Program, *IEEE J. Sel. Top.*  
 1063 *Appl.*, 2, 144-162, 10.1109/jstars.2009.2027443, 2009.  
 1064  
 1065 Reid, J. S., Xian, P., Hyer, E. J., Flatau, M. K., Ramirez, E. M., Turk, F. J., Sampson, C. R.,  
 1066 Zhang, C., Fukada, E. M., and Maloney, E. D.: Multi-scale meteorological conceptual analysis of  
 1067 observed active fire hotspot activity and smoke optical depth in the Maritime Continent, *Atmos.*  
 1068 *Chem. Phys.*, 12, 2117-2147, 10.5194/acp-12-2117-2012, 2012.  
 1069  
 1070 Reid, J. S., Hyer, E. J., Johnson, R. S., Holben, B. N., Yokelson, R. J., Zhang, J., Campbell, J. R.,  
 1071 Christopher, S. A., Di Girolamo, L., Giglio, L., Holz, R. E., Kearney, C., Miettinen, J., Reid, E.  
 1072 A., Turk, F. J., Wang, J., Xian, P., Zhao, G., Balasubramanian, R., Chew, B. N., Janjai, S.,  
 1073 Lagrosas, N., Lestari, P., Lin, N.-H., Mahmud, M., Nguyen, A. X., Norris, B., Oanh, N. T. K.,  
 1074 Oo, M., Salinas, S. V., Welton, E. J., and Liew, S. C.: Observing and understanding the  
 1075 Southeast Asian aerosol system by remote sensing: An initial review and analysis for the Seven  
 1076 Southeast Asian Studies (7SEAS) program, *Atmos. Res.*, 122, 403-468,  
 1077 <https://doi.org/10.1016/j.atmosres.2012.06.005>, 2013.  
 1078  
 1079 Reid, J. S., Lagrosas, N. D., Jonsson, H. H., Reid, E. A., Sessions, W. R., Simpas, J. B., Uy, S.  
 1080 N., Boyd, T. J., Atwood, S. A., Blake, D. R., Campbell, J. R., Cliff, S. S., Holben, B. N., Holz,  
 1081 R. E., Hyer, E. J., Lynch, P., Meinardi, S., Posselt, D. J., Richardson, K. A., Salinas, S. V.,  
 1082 Smirnov, A., Wang, Q., Yu, L., and Zhang, J.: Observations of the temporal variability in aerosol  
 1083 properties and their relationships to meteorology in the summer monsoonal South China Sea/East  
 1084 Sea: the scale-dependent role of monsoonal flows, the Madden–Julian Oscillation, tropical  
 1085 cyclones, squall lines and cold pools, *Atmos. Chem. Phys.*, 15, 1745-1768, 10.5194/acp-15-  
 1086 1745-2015, 2015.  
 1087  
 1088 Reid, J. S., Xian, P., Holben, B. N., Hyer, E. J., Reid, E. A., Salinas, S. V., Zhang, J., Campbell,  
 1089 J. R., Chew, B. N., Holz, R. E., Kuciauskas, A. P., Lagrosas, N., Posselt, D. J., Sampson, C. R.,  
 1090 Walker, A. L., Welton, E. J., and Zhang, C.: Aerosol meteorology of the Maritime Continent for  
 1091 the 2012 7SEAS southwest monsoon intensive study – Part 1: regional-scale phenomena, *Atmos.*  
 1092 *Chem. Phys.*, 16, 14041-14056, 10.5194/acp-16-14041-2016, 2016a.  
 1093  
 1094 Reid, J. S., Lagrosas, N. D., Jonsson, H. H., Reid, E. A., Atwood, S. A., Boyd, T. J., Ghate, V.  
 1095 P., Xian, P., Posselt, D. J., Simpas, J. B., Uy, S. N., Zaiger, K., Blake, D. R., Bucholtz, A.,  
 1096 Campbell, J. R., Chew, B. N., Cliff, S. S., Holben, B. N., Holz, R. E., Hyer, E. J., Kreidenweis,  
 1097 S. M., Kuciauskas, A. P., Lolli, S., Oo, M., Perry, K. D., Salinas, S. V., Sessions, W. R.,  
 1098 Smirnov, A., Walker, A. L., Wang, Q., Yu, L., Zhang, J., and Zhao, Y.: Aerosol meteorology of  
 1099 Maritime Continent for the 2012 7SEAS southwest monsoon intensive study – Part 2: Philippine  
 1100 receptor observations of fine-scale aerosol behavior, *Atmos. Chem. Phys.*, 16, 14057-14078,  
 1101 10.5194/acp-16-14057-2016, 2016b.  
 1102

1103 Ross, A. D., Holz, R. E., Quinn, G., Reid, J. S., Xian, P., Turk, F. J., and Posselt, D. J.: Exploring  
1104 the first aerosol indirect effect over Southeast Asia using a 10-year collocated MODIS, CALIOP,  
1105 and model dataset, *Atmos. Chem. Phys.*, 18, 12747-12764, 10.5194/acp-18-12747-2018, 2018.  
1106

1107 Satsumabayashi, H., Kurita, H., Yokouchi, Y., and Ueda, H.: Photochemical formation of  
1108 particulate dicarboxylic acids under long-range transport in central Japan, *Atmos. Environ.. Part*  
1109 *A. General Topics*, 24, 1443-1450, [https://doi.org/10.1016/0960-1686\(90\)90053-P](https://doi.org/10.1016/0960-1686(90)90053-P), 1990.  
1110

1111 Schlosser, J. S., Braun, R. A., Bradley, T., Dadashazar, H., MacDonald, A. B., Aldhaif, A. A.,  
1112 Aghdam, M. A., Mardi, A. H., Xian, P., and Sorooshian, A.: Analysis of aerosol composition  
1113 data for western United States wildfires between 2005 and 2015: Dust emissions, chloride  
1114 depletion, and most enhanced aerosol constituents, *J. Geophys. Res.-Atmos.*, 122, 8951-8966,  
1115 10.1002/2017jd026547, 2017.  
1116

1117 Simpas, J., Lorenzo, G., and Cruz, M. T.: Monitoring Particulate Matter Levels and Composition  
1118 for Source Apportionment Study in Metro Manila, Philippines, in: *Improving Air Quality in*  
1119 *Asian Developing Countries: Compilation of Research Findings*, edited by: Kim Oanh, N. T.,  
1120 NARENCA, Vietnam Publishing House of Natural Resources, Environment and Cartography,  
1121 Vietnam, 239-261, 2014.  
1122

1123 Singh, M., Jaques, P. A., and Sioutas, C.: Size distribution and diurnal characteristics of particle-  
1124 bound metals in source and receptor sites of the Los Angeles Basin, *Atmos. Environ.*, 36, 1675-  
1125 1689, [https://doi.org/10.1016/S1352-2310\(02\)00166-8](https://doi.org/10.1016/S1352-2310(02)00166-8), 2002.  
1126

1127 Song, J., Zhao, Y., Zhang, Y., Fu, P., Zheng, L., Yuan, Q., Wang, S., Huang, X., Xu, W., Cao,  
1128 Z., Gromov, S., and Lai, S.: Influence of biomass burning on atmospheric aerosols over the  
1129 western South China Sea: Insights from ions, carbonaceous fractions and stable carbon isotope  
1130 ratios, *Environ. Pollut.*, 242, 1800-1809, <https://doi.org/10.1016/j.envpol.2018.07.088>, 2018.  
1131

1132 Song, X.-H., Polissar, A. V., and Hopke, P. K.: Sources of fine particle composition in the  
1133 northeastern US, *Atmos. Environ.*, 35, 5277-5286, [https://doi.org/10.1016/S1352-](https://doi.org/10.1016/S1352-2310(01)00338-7)  
1134 [2310\(01\)00338-7](https://doi.org/10.1016/S1352-2310(01)00338-7), 2001.  
1135

1136 Sorooshian, A., Varutbangkul, V., Brechtel, F. J., Ervens, B., Feingold, G., Bahreini, R.,  
1137 Murphy, S. M., Holloway, J. S., Atlas, E. L., Buzorius, G., Jonsson, H., Flagan, R. C., and  
1138 Seinfeld, J. H.: Oxalic acid in clear and cloudy atmospheres: Analysis of data from International  
1139 Consortium for Atmospheric Research on Transport and Transformation 2004, *J. Geophys. Res.-*  
1140 *Atmos.*, 111, 10.1029/2005jd006880, 2006.  
1141

1142 Sorooshian, A., Ng, N. L., Chan, A. W. H., Feingold, G., Flagan, R. C., and Seinfeld, J. H.:  
1143 Particulate organic acids and overall water-soluble aerosol composition measurements from the  
1144 2006 Gulf of Mexico Atmospheric Composition and Climate Study (GoMACCS), *J. Geophys.*  
1145 *Res.-Atmos.*, 112, 10.1029/2007jd008537, 2007a.  
1146

1147 Sorooshian, A., Lu, M.-L., Brechtel, F. J., Jonsson, H., Feingold, G., Flagan, R. C., and Seinfeld,  
1148 J. H.: On the Source of Organic Acid Aerosol Layers above Clouds, *Environ. Sci. Technol.*, 41,  
1149 4647-4654, 10.1021/es0630442, 2007b.

1150

1151 Sorooshian, A., Crosbie, E., Maudlin, L. C., Youn, J.-S., Wang, Z., Shingler, T., Ortega, A. M.,  
1152 Hersey, S., and Woods, R. K.: Surface and airborne measurements of organosulfur and  
1153 methanesulfonate over the western United States and coastal areas, *J. Geophys. Res.-Atmos.*,  
1154 120, 8535-8548, 10.1002/2015jd023822, 2015.

1155

1156 Stein, A. F., Draxler, R. R., Rolph, G. D., Stunder, B. J. B., Cohen, M. D., and Ngan, F.:  
1157 NOAA's HYSPLIT Atmospheric Transport and Dispersion Modeling System, *B. Am. Meteorol.*  
1158 *Soc.*, 96, 2059-2077, 10.1175/bams-d-14-00110.1, 2015.

1159

1160 Sternbeck, J., Sjödin, Å., and Andréasson, K.: Metal emissions from road traffic and the  
1161 influence of resuspension—results from two tunnel studies, *Atmos. Environ.*, 36, 4735-4744,  
1162 [https://doi.org/10.1016/S1352-2310\(02\)00561-7](https://doi.org/10.1016/S1352-2310(02)00561-7), 2002.

1163

1164 Thepnuan, D., Chantara, S., Lee, C.-T., Lin, N.-H., and Tsai, Y. I.: Molecular markers for  
1165 biomass burning associated with the characterization of PM<sub>2.5</sub> and component sources during  
1166 dry season haze episodes in Upper South East Asia, *Sci. Total Environ.*, 658, 708-722,  
1167 <https://doi.org/10.1016/j.scitotenv.2018.12.201>, 2019.

1168

1169 Thurston, G. D., and Spengler, J. D.: A quantitative assessment of source contributions to  
1170 inhalable particulate matter pollution in metropolitan Boston, *Atmos. Environ.*, 19, 9-25,  
1171 [https://doi.org/10.1016/0004-6981\(85\)90132-5](https://doi.org/10.1016/0004-6981(85)90132-5), 1985.

1172

1173 Vaughan, M. A., Young, S. A., Winker, D. M., Powell, K. A., Omar, A. H., Liu, Z., Hu, Y., and  
1174 Hostetler, C. A.: Fully automated analysis of space-based lidar data: an overview of the  
1175 CALIPSO retrieval algorithms and data products, *Proc. SPIE*, 5575,  
1176 <https://doi.org/10.1117/12.572024>, 2004.

1177

1178 Wang, H., and Shooter, D.: Low molecular weight dicarboxylic acids in PM<sub>10</sub> in a city with  
1179 intensive solid fuel burning, *Chemosphere*, 56, 725-733,  
1180 <https://doi.org/10.1016/j.chemosphere.2004.04.030>, 2004.

1181

1182 Wang, J., Ge, C., Yang, Z., Hyer, E. J., Reid, J. S., Chew, B.-N., Mahmud, M., Zhang, Y., and  
1183 Zhang, M.: Mesoscale modeling of smoke transport over the Southeast Asian Maritime  
1184 Continent: Interplay of sea breeze, trade wind, typhoon, and topography, *Atmos. Res.*, 122, 486-  
1185 503, <https://doi.org/10.1016/j.atmosres.2012.05.009>, 2013.

1186

1187 Wang, S.-H., Tsay, S.-C., Lin, N.-H., Hsu, N. C., Bell, S. W., Li, C., Ji, Q., Jeong, M.-J.,  
1188 Hansell, R. A., Welton, E. J., Holben, B. N., Sheu, G.-R., Chu, Y.-C., Chang, S.-C., Liu, J.-J.,  
1189 and Chiang, W.-L.: First detailed observations of long-range transported dust over the northern  
1190 South China Sea, *Atmos. Environ.*, 45, 4804-4808,  
1191 <https://doi.org/10.1016/j.atmosenv.2011.04.077>, 2011.

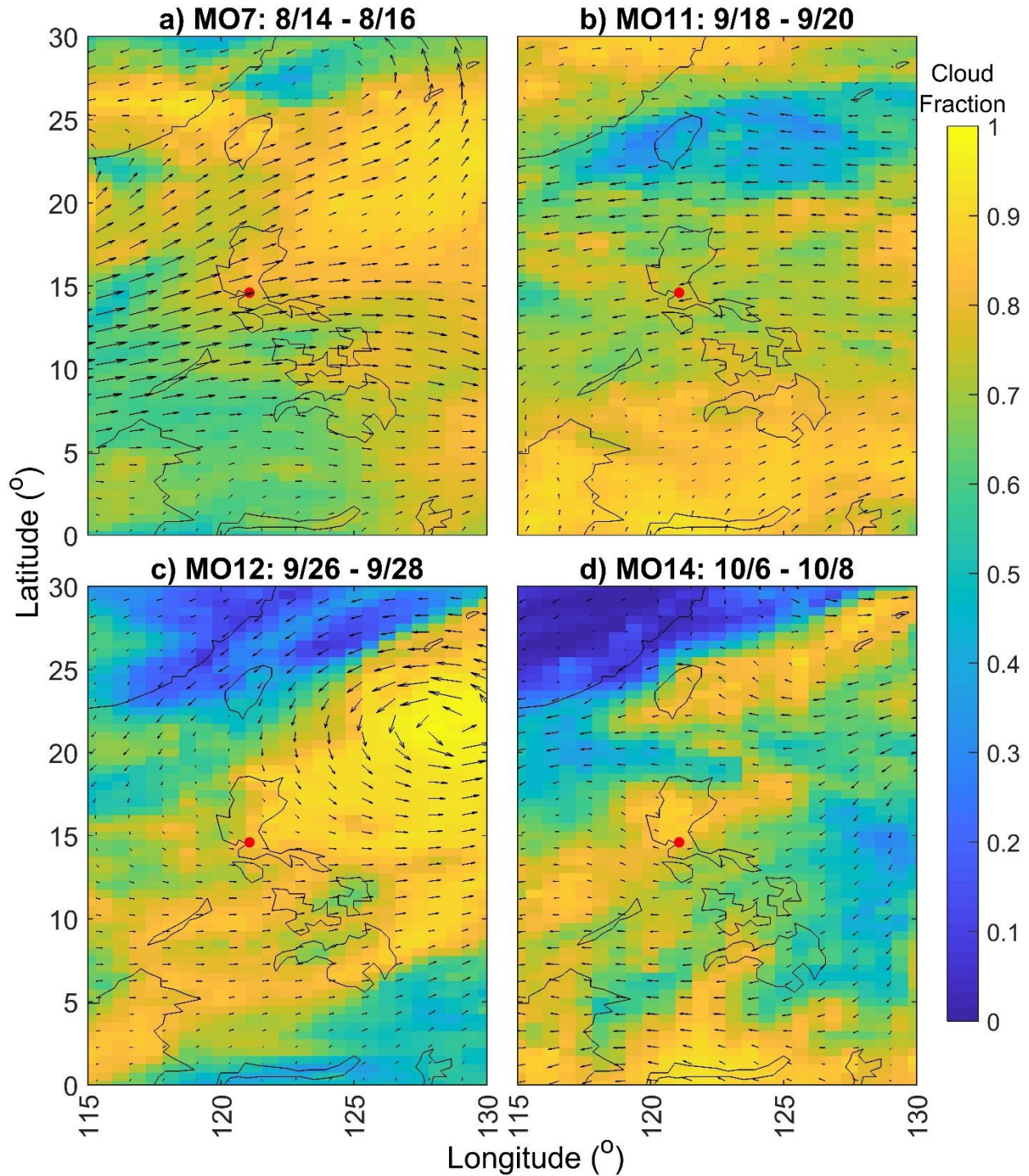
1192

1193 Weber, R. J., Sullivan, A. P., Peltier, R. E., Russell, A., Yan, B., Zheng, M., de Gouw, J.,  
1194 Warneke, C., Brock, C., Holloway, J. S., Atlas, E. L., and Edgerton, E.: A study of secondary  
1195 organic aerosol formation in the anthropogenic-influenced southeastern United States, *J.*  
1196 *Geophys. Res.-Atmos.*, 112, 10.1029/2007jd008408, 2007.  
1197  
1198 Wen, H., and Carignan, J.: Reviews on atmospheric selenium: Emissions, speciation and fate,  
1199 *Atmos. Environ.*, 41, 7151-7165, <https://doi.org/10.1016/j.atmosenv.2007.07.035>, 2007.  
1200  
1201 Winker, D. M., Vaughan, M. A., Omar, A., Hu, Y., Powell, K. A., Liu, Z., Hunt, W. H., and  
1202 Young, S. A.: Overview of the CALIPSO Mission and CALIOP Data Processing Algorithms, *J.*  
1203 *Atmos. Ocean. Tech.*, 26, 2310-2323, 10.1175/2009jtecha1281.1, 2009.  
1204  
1205 Wonaschuetz, A., Sorooshian, A., Ervens, B., Chuang, P. Y., Feingold, G., Murphy, S. M., de  
1206 Gouw, J., Warneke, C., and Jonsson, H. H.: Aerosol and gas re-distribution by shallow cumulus  
1207 clouds: An investigation using airborne measurements, *J. Geophys. Res.-Atmos.*, 117,  
1208 10.1029/2012jd018089, 2012.  
1209  
1210 Xian, P., Reid, J. S., Atwood, S. A., Johnson, R. S., Hyer, E. J., Westphal, D. L., and Sessions,  
1211 W.: Smoke aerosol transport patterns over the Maritime Continent, *Atmos. Res.*, 122, 469-485,  
1212 <https://doi.org/10.1016/j.atmosres.2012.05.006>, 2013.  
1213  
1214 Xu, J., Zhang, J., Liu, J., Yi, K., Xiang, S., Hu, X., Wang, Y., Tao, S., and Ban-Weiss, G.:  
1215 Influence of cloud microphysical processes on black carbon wet removal, global distributions,  
1216 and radiative forcing, *Atmos. Chem. Phys.*, 19, 1587-1603, 10.5194/acp-19-1587-2019, 2019.  
1217  
1218 Yamasoe, M. A., Artaxo, P., Miguel, A. H., and Allen, A. G.: Chemical composition of aerosol  
1219 particles from direct emissions of vegetation fires in the Amazon Basin: water-soluble species  
1220 and trace elements, *Atmos. Environ.*, 34, 1641-1653, [https://doi.org/10.1016/S1352-](https://doi.org/10.1016/S1352-2310(99)00329-5)  
1221 [2310\(99\)00329-5](https://doi.org/10.1016/S1352-2310(99)00329-5), 2000.  
1222  
1223 Yan, J., Chen, L., Lin, Q., Zhao, S., and Zhang, M.: Effect of typhoon on atmospheric aerosol  
1224 particle pollutants accumulation over Xiamen, China, *Chemosphere*, 159, 244-255,  
1225 <https://doi.org/10.1016/j.chemosphere.2016.06.006>, 2016.  
1226  
1227 Yao, X., Fang, M., Chan, C. K., Ho, K. F., and Lee, S. C.: Characterization of dicarboxylic acids  
1228 in PM<sub>2.5</sub> in Hong Kong, *Atmos. Environ.*, 38, 963-970,  
1229 <https://doi.org/10.1016/j.atmosenv.2003.10.048>, 2004.  
1230  
1231 Yokelson, R. J., Crouse, J. D., DeCarlo, P. F., Karl, T., Urbanski, S., Atlas, E., Campos, T.,  
1232 Shinozuka, Y., Kapustin, V., Clarke, A. D., Weinheimer, A., Knapp, D. J., Montzka, D. D.,  
1233 Holloway, J., Weibring, P., Flocke, F., Zheng, W., Toohey, D., Wennberg, P. O., Wiedinmyer,  
1234 C., Mauldin, L., Fried, A., Richter, D., Walega, J., Jimenez, J. L., Adachi, K., Buseck, P. R.,  
1235 Hall, S. R., and Shetter, R.: Emissions from biomass burning in the Yucatan, *Atmos. Chem.*  
1236 *Phys.*, 9, 5785-5812, 10.5194/acp-9-5785-2009, 2009.  
1237

1238 Zhang, Y.-N., Zhang, Z.-S., Chan, C.-Y., Engling, G., Sang, X.-F., Shi, S., and Wang, X.-M.:  
1239 Levoglucosan and carbonaceous species in the background aerosol of coastal southeast China:  
1240 case study on transport of biomass burning smoke from the Philippines, *Environ. Sci. Pollut. R.*,  
1241 19, 244-255, 10.1007/s11356-011-0548-7, 2012.  
1242  
1243 Zhao, X., Wang, X., Ding, X., He, Q., Zhang, Z., Liu, T., Fu, X., Gao, B., Wang, Y., Zhang, Y.,  
1244 Deng, X., and Wu, D.: Compositions and sources of organic acids in fine particles (PM<sub>2.5</sub>) over  
1245 the Pearl River Delta region, south China, *J. Environ. Sci.*, 26, 110-121,  
1246 [https://doi.org/10.1016/S1001-0742\(13\)60386-1](https://doi.org/10.1016/S1001-0742(13)60386-1), 2014.

1247 **Table 1.** Description of the MOUDI sample sets from this study. Accumulated precipitation  
 1248 during the sample sets was found using PERSIANN-CCS for the area bounded by: 121.0199 -  
 1249 121.0968° E and 14.6067 - 14.6946° N.  
 1250

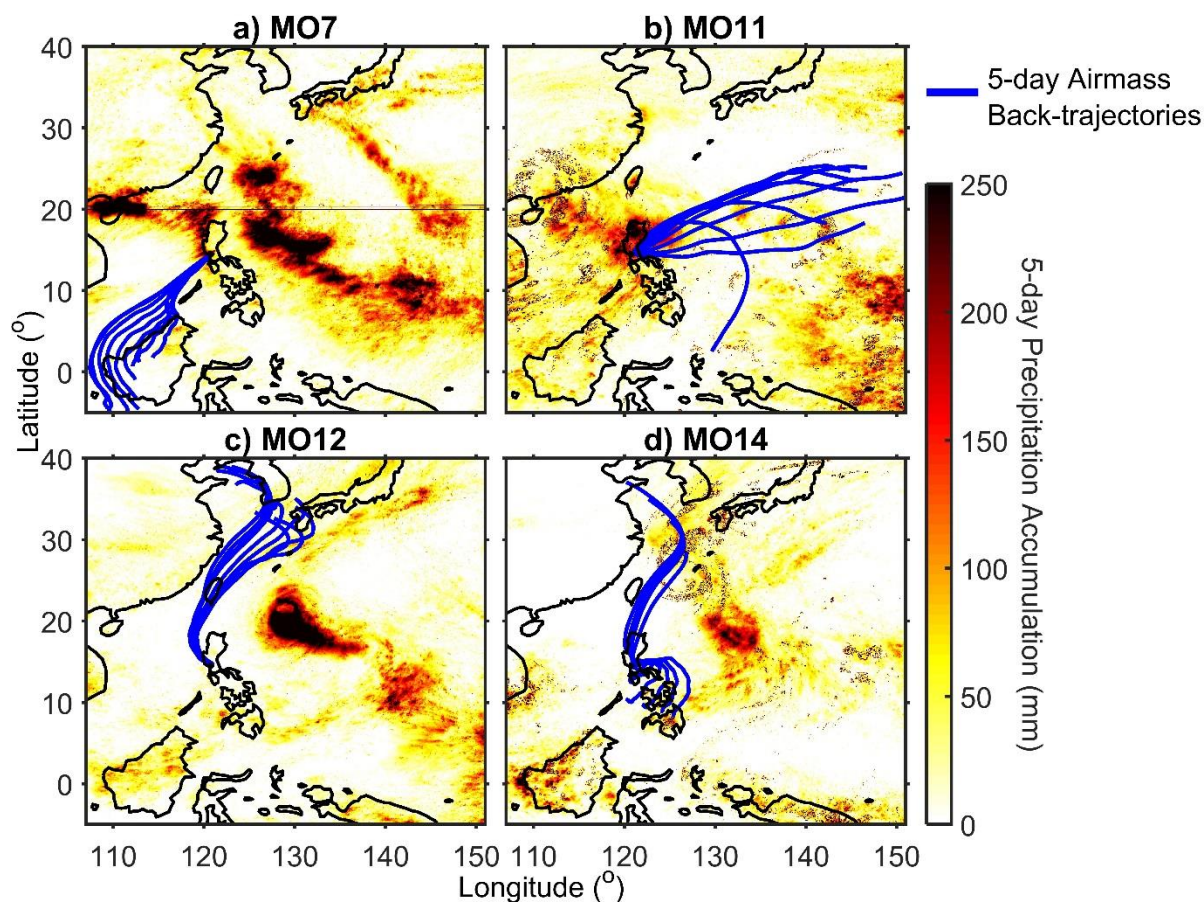
Set Name	Start Date/ Local Time	End Date/ Local Time	Total Water-Soluble Species ( $\mu\text{g m}^{-3}$ )	% of water- soluble mass < 1 $\mu\text{m}$	Precipitation (mm)
MO1	7/19/18 12:40 PM	7/20/18 12:43 PM	4.61	67.3%	27
MO2	7/23/18 11:29 AM	7/25/18 5:10 PM	6.52	62.1%	14
MO4	7/25/18 7:16 PM	7/30/18 6:12 PM	5.17	66.4%	35
MO5	7/30/18 7:17 PM	8/1/18 1:19 PM	9.17	64.8%	11
MO6	8/6/18 2:33 PM	8/8/18 2:38 PM	5.11	55.8%	50
MO7	8/14/18 1:59 PM	8/16/18 2:04 PM	13.70	60.3%	3
MO8	8/22/18 1:46 PM	8/24/18 1:53 PM	12.73	71.6%	10
MO9	9/1/18 5:00 AM	9/3/18 5:05 AM	6.23	76.7%	64
MO10	9/10/18 2:42 PM	9/12/18 3:02 PM	6.36	79.5%	20
MO11	9/18/18 2:12 PM	9/20/18 2:24 PM	2.70	47.3%	26
MO12	9/26/18 1:53 PM	9/28/18 1:53 PM	13.49	59.9%	1
MO14	10/6/18 5:00 AM	10/8/18 5:05 AM	16.55	78.4%	0



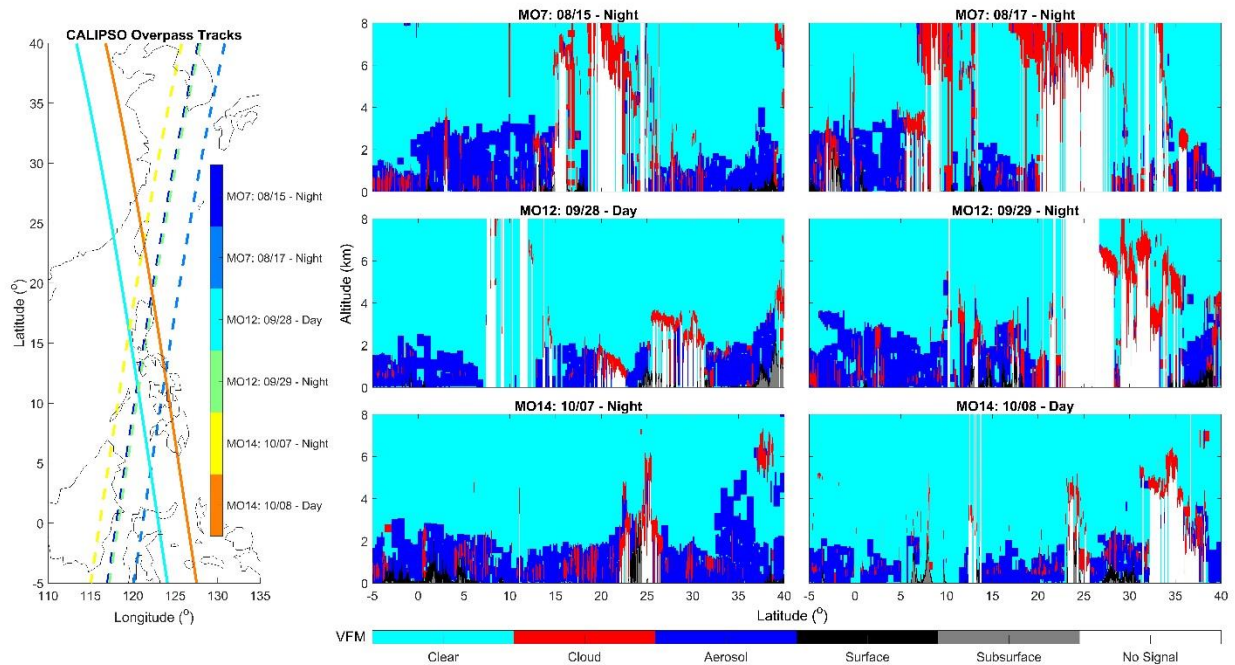
1251  
 1252  
 1253  
 1254  
 1255  
 1256

**Figure 1.** MERRA-2 data for 850 hPa wind vectors and total cloud fraction averaged over the sample set duration for a) MO7 (8/14 – 8/16), b) MO11 (9/18 – 9/20), c) MO12 (9/26 – 9/28), and d) MO14 (10/6 – 10/8). The location of the Manila Observatory is indicated by the red circle. (Note that 850 hPa wind vectors are also averaged to increase grid spacing and improve figure readability.)



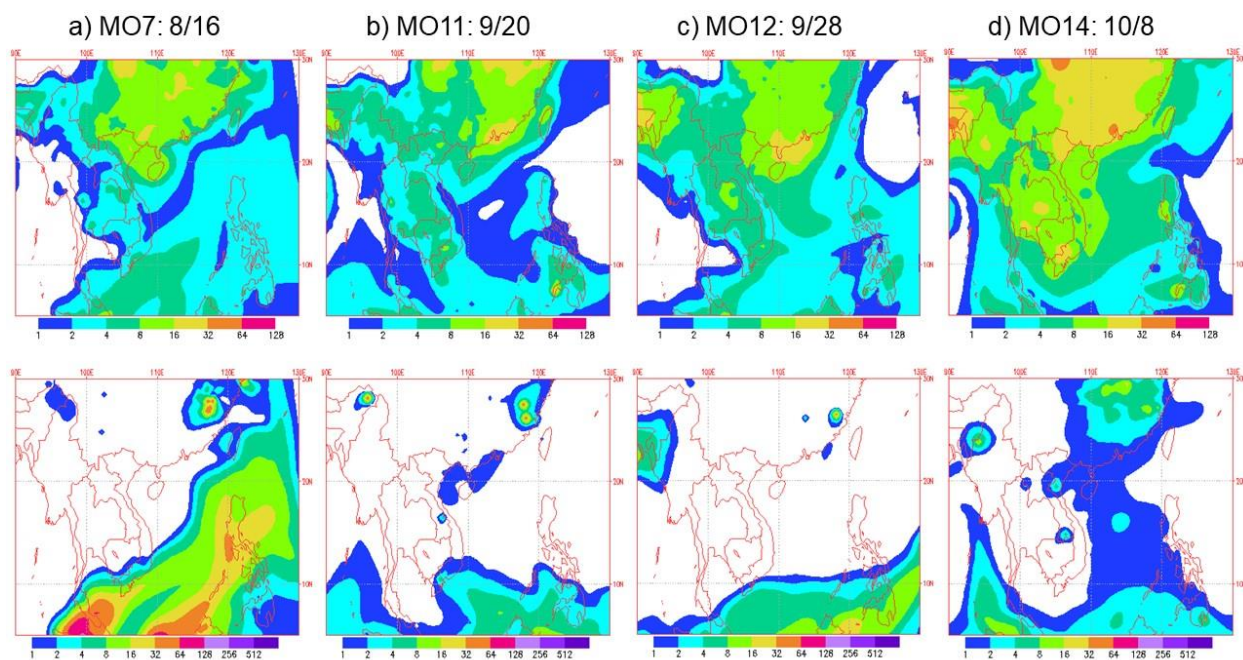


1257  
 1258 **Figure 2.** Rainfall accumulation, extending from 5 days before the midpoint of each sample set  
 1259 until the midpoint of each sample set, from PERSIAN-CCS for a) MO7, b) MO11, c) MO12, and  
 1260 d) MO14. In blue are the 5-day air mass back-trajectories terminating at the MOUDI inlet at MO  
 1261 (~85 m above sea level) every 6 h during each of the sample study periods. Note that the  
 1262 maximum precipitation accumulation in the region shown during the study periods was 955 mm;  
 1263 however, for figure readability, the scale was reduced to 0-250 mm.

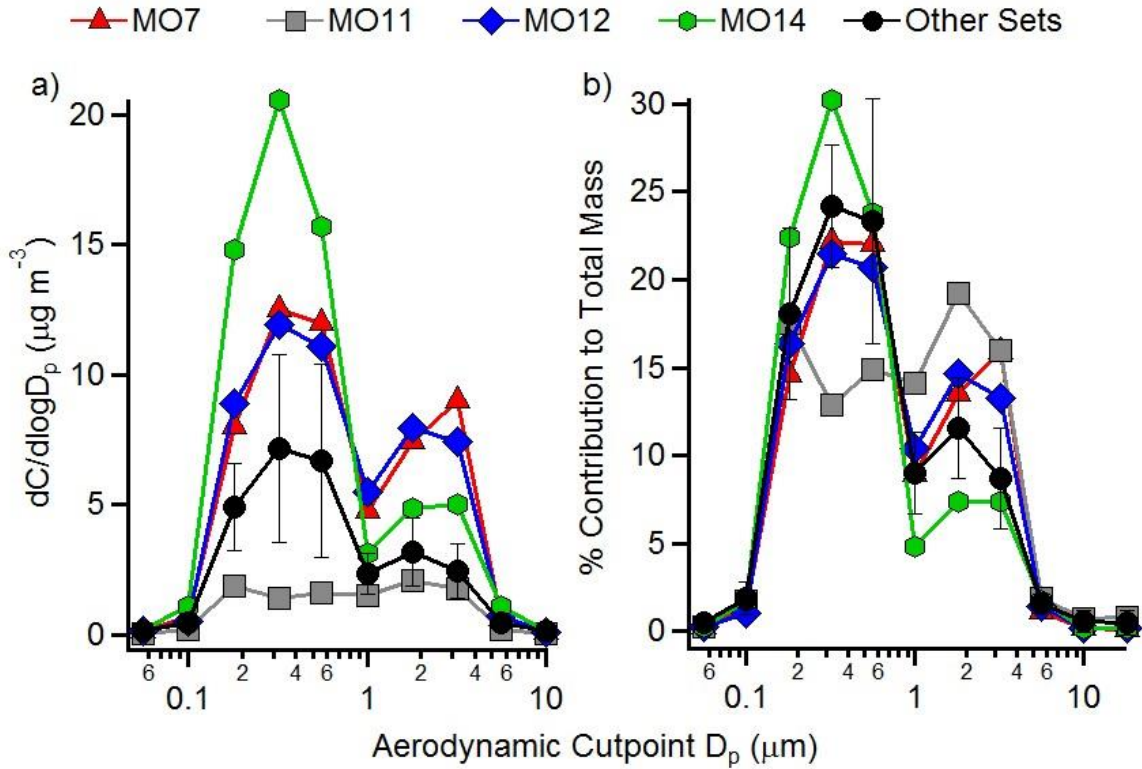


1264  
 1265  
 1266  
 1267  
 1268  
 1269  
 1270

**Figure 3.** CALIOP Vertical Feature Mask (VFM) for overpasses during or following MO7, MO12, and MO14. For the CALIPSO satellite overpass tracks, the dashed lines correspond to the nighttime profiles and solid lines are for daytime. Note that nighttime overpasses correspond to early morning times before sunrise for the listed days and daytime overpasses occurred during early afternoon.

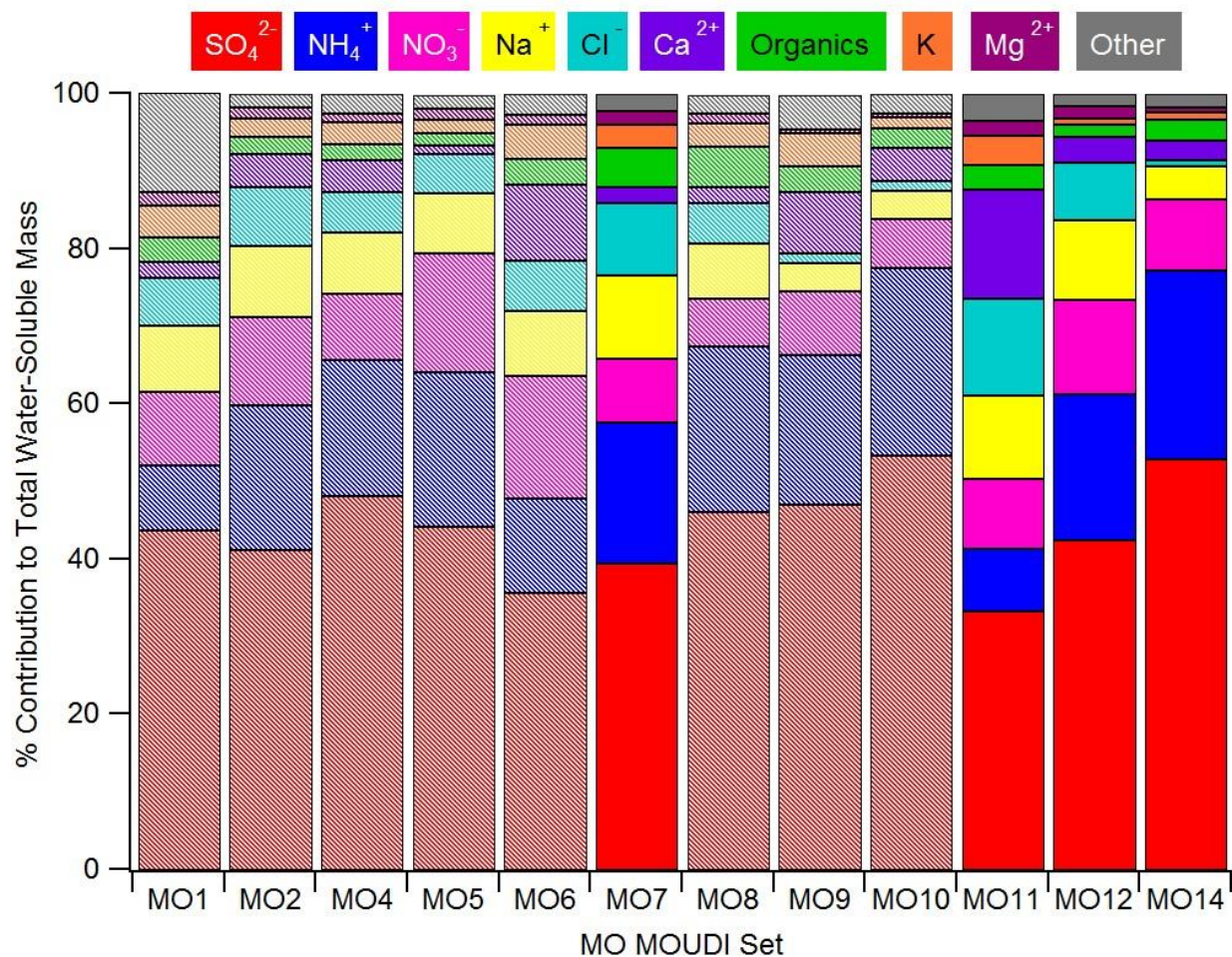


1271  
 1272 **Figure 4.** NAAPS model snapshots corresponding to conditions at the stop time of sample sets a)  
 1273 MO7, b) MO11, and c) MO12 and d) 3 h after the sample stop time for MO14. The top row of  
 1274 figures is anthropogenic and biogenic fine aerosol (ABF) surface concentration ( $\mu\text{g m}^{-3}$ ), while  
 1275 the bottom row is biomass burning smoke surface concentration ( $\mu\text{g m}^{-3}$ ).

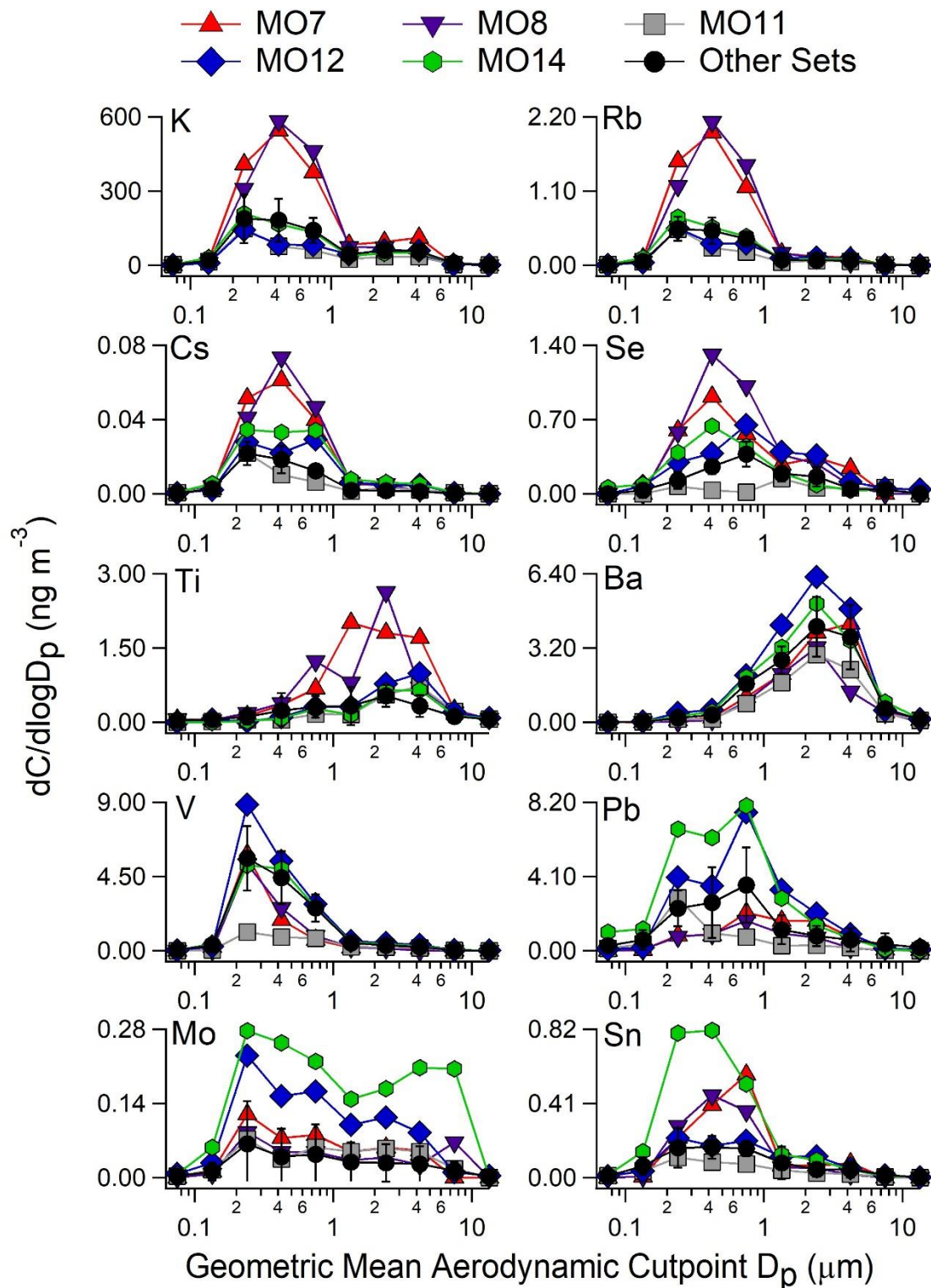


1276  
 1277  
 1278  
 1279  
 1280  
 1281  
 1282

**Figure 5.** a) Mass size distributions for total water-soluble mass ( $C =$  sum of mass concentrations for water-soluble species) and b) percent contribution of each size range to the total water-soluble mass for the three MOUDI sets with the highest aerosol mass concentrations (MO7, MO12, and MO14), the set with the lowest concentration (MO11), and the average ( $\pm$  one standard deviation error bars) for the remaining eight sets.

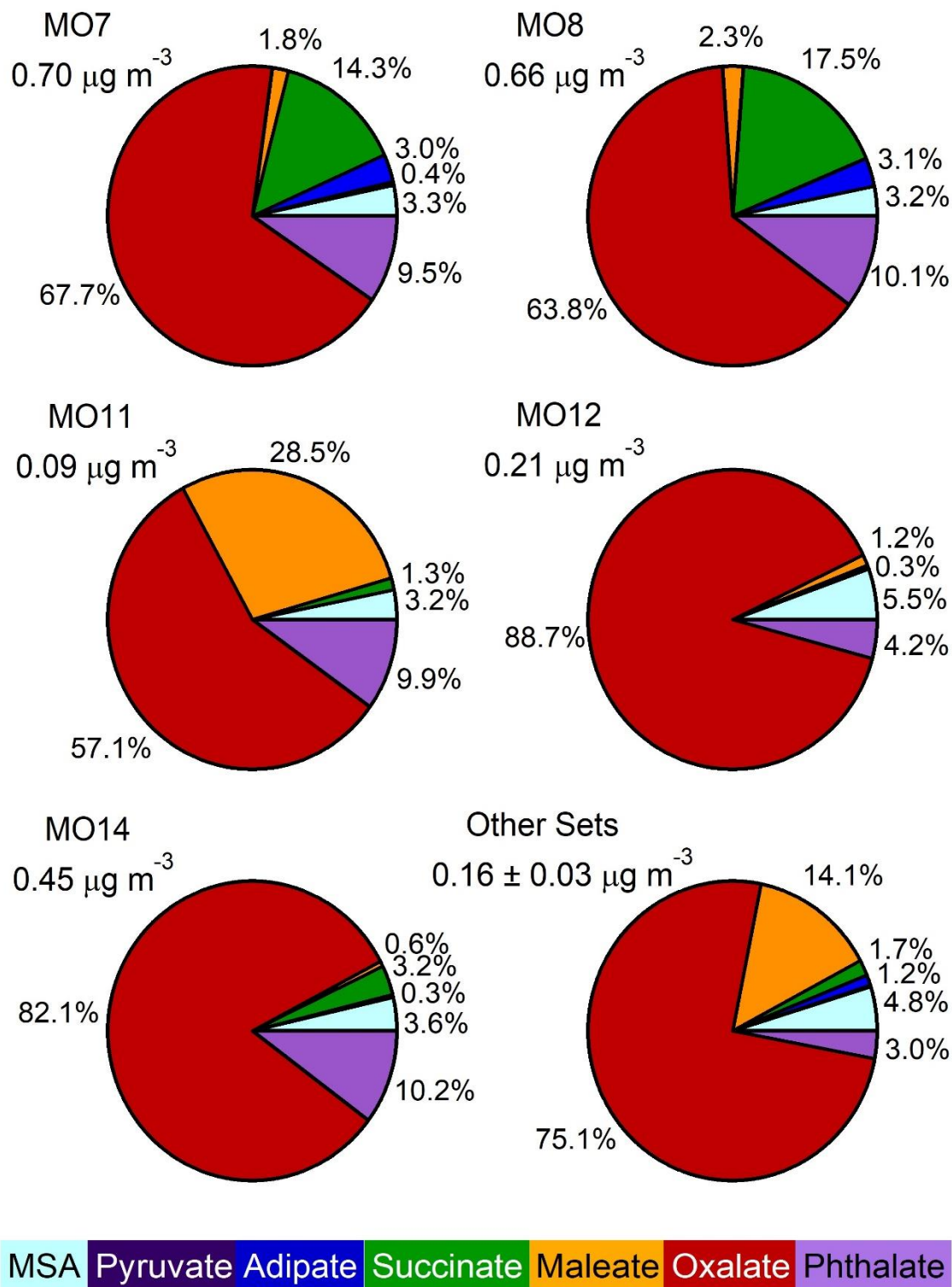


1283  
 1284 **Figure 6.** Percent contribution of various species to the total water-soluble mass concentration  
 1285 for each of the 12 sample sets. The sample sets with the three highest aerosol concentrations  
 1286 (MO7, MO12, and MO14) and the lowest aerosol concentration (MO11) are shown as solid bars  
 1287 while all other sample sets are stripes. The “organics” category contains the sum of  
 1288 methanesulfonate (MSA), pyruvate, adipate, succinate, maleate, oxalate, and phthalate.



1289  
 1290  
 1291  
 1292  
 1293

**Figure 7.** Selected elements that showed elevated concentrations during at least one of the highest aerosol events (MO7, MO8, MO12, or MO14). The concentrations from the lowest aerosol event (MO11) are also shown. The “other sets” category displays the average ( $\pm$  one standard deviation) for the remaining seven sets.



1294  
1295  
1296  
1297  
1298  
1299

**Figure 8.** Pie charts showing the fraction of species contributing to the measured water-soluble organic aerosol. Below each pie chart title is the sum of the water-soluble organic species measured, with the “other sets” chart showing the average  $\pm$  one standard deviation for the remaining sets. Acronyms: Methanesulfonate (MSA)